

1 **Few fixed variants between trophic specialist pupfish species**
2 **reveal candidate *cis*-regulatory alleles underlying rapid**
3 **craniofacial divergence**

4 Joseph A. McGirr¹, Christopher H. Martin²

5
6
7
8
9

10
11
12
13
14

15 ¹Environmental Toxicology Department, University of California, Davis, CA 95616

16 ²Department of Integrative Biology and Museum of Vertebrate Zoology, University of
17 California, Berkeley, CA 94720

18 Running Title: *Cis*-regulatory alleles underlying craniofacial divergence

19 Keywords: RNAseq, F1 hybrid, trophic specialization, allele specific expression, adaptive
20 radiation, ecological speciation

21 Correspondence: Christopher Martin

22 Email: chmartin@berkeley.edu

23 Word count abstract: 246; Word count main text: 7,217; Figures: 8; Tables: 1.

24 **Abstract**

25 Investigating closely related species that rapidly evolved divergent feeding morphology is a
26 powerful approach to identify genetic variation underlying variation in complex traits. This can
27 also lead to the discovery of novel candidate genes influencing natural and clinical variation in
28 human craniofacial phenotypes. We combined whole-genome resequencing of 258 individuals
29 with 50 transcriptomes to identify candidate *cis*-acting genetic variation underlying rapidly
30 evolving craniofacial phenotypes within an adaptive radiation of *Cyprinodon* pupfishes. This
31 radiation consists of a dietary generalist species and two derived trophic niche specialists – a
32 molluscivore and a scale-eating species. Despite extensive morphological divergence, these
33 species only diverged 10 kya and produce fertile hybrids in the laboratory. Out of 9.3 million
34 genome-wide SNPs and 80,012 structural variants, we found very few alleles fixed between
35 species – only 157 SNPs and 87 deletions. Comparing gene expression across 38 purebred F1
36 offspring sampled at three early developmental stages, we identified 17 fixed variants within 10
37 kilobases of 12 genes that were highly differentially expressed between species. By measuring
38 allele-specific expression in F1 hybrids from multiple crosses, we found that the majority of
39 expression divergence between species was explained by *trans*-regulatory mechanisms. We also
40 found strong evidence for two *cis*-regulatory alleles affecting expression divergence of two genes
41 with putative effects on skeletal development (*dync2li1* and *pycr3*). These results suggest that
42 SNPs and structural variants contribute to the evolution of novel traits and highlight the utility of
43 the San Salvador Island pupfish system as an evolutionary model for craniofacial development.

44

45

46

47

48

49

50

51

52

53

54

55 **Introduction**

56 Developing a mechanistic understanding of genetic variation contributing to variation in
57 complex craniofacial traits is a major goal of both basic and translational research. This involves
58 identifying genetic variants influencing natural morphological diversity as well as craniofacial
59 anomalies, which account for approximately one-third of all birth defects (Gorlin et al. 1990). It
60 is now understood that much of the natural and clinical variation in complex traits like
61 craniofacial morphology results from interactions among hundreds to thousands of loci across
62 the genome (Boyle et al. 2017; Sella et al. 2019). Genome-wide association studies (GWAS)
63 have shown that the vast majority of genetic variants affecting complex traits and diseases are
64 within non-coding regions, highlighting the importance of gene regulation influencing trait
65 variation (Hindorff et al. 2009; Maurano et al. 2012; Schaub et al. 2012). However, much of
66 what is currently known about the developmental genetic basis of craniofacial diversity comes
67 from mutagenesis screens and loss of function experiments in model organisms. These types of
68 experiments are biased to detect alleles within protein-coding regions that severely disrupt gene
69 function and are likely to cause lethality at early developmental stages (Nguyen and Tian 2008;
70 Hall 2009). Thus, complementary approaches to mutagenesis screens are necessary to identify
71 genes that influence craniofacial phenotypes at later stages in development through changes in
72 gene regulation rather than gene function.

73 One such approach is to harness naturally occurring genetic variation between
74 ‘evolutionary mutants’ – closely related species exhibiting divergent phenotypes that mimic
75 human disease phenotypes (Albertson et al. 2008). Several fish systems have been particularly
76 useful as models for craniofacial developmental disorders because closely related species are
77 often distinguished by differences in morphological traits important for trophic niche
78 specialization, such as the shape and dynamics of jaws and pharyngeal elements (Albertson et al.
79 2008; Schartl 2014; Powder and Albertson 2016). The process of identifying candidate genes and
80 validating their effect on phenotypic divergence in evolutionary mutants typically involves
81 population genomic analyses, gene expression analyses, GWAS, and functional validation
82 experiments (Bono et al. 2015; Kratochwil and Meyer 2015). Using a combination of these
83 approaches, research in fish systems has shown that the evolution of adaptive craniofacial traits
84 often involve orthologs of genes implicated in human disorders (Albertson et al. 2005; Helms et
85 al. 2005; Roberts et al. 2011; Ahi et al. 2014; Cleves et al. 2014; Lencer et al. 2017; Erickson et

86 al. 2018; Gross and Powers 2018; Martin et al. 2019). Therefore, candidate genes identified in
87 evolutionary mutant models that have orthologs with uncharacterized functions in humans
88 warrant further study into their relationship with development and disease.

89 Measuring relative and absolute genetic differentiation (estimated as *Fst* and *Dxy*)
90 between species can reveal diverged regions of the genome that may influence trait development,
91 but these statistics alone are insufficient to identify genetic mechanisms underlying evolutionary
92 mutant phenotypes (Nachman and Payseur 2012; Cruickshank and Hahn 2014). RNA sequencing
93 across multiple developmental stages and tissue types can provide further evidence that
94 differentiated regions influence phenotypic divergence if genes near genetic variants are
95 differentially expressed between species (Whiteley et al. 2010; Poelstra et al. 2014; McGirr and
96 Martin 2018; Verta and Jones 2019). However, this assumes that linked genetic variation within
97 *cis*-acting regulatory elements affects proximal gene expression levels, and does not rule out the
98 possibility of unlinked *trans*-acting regulatory variation binding regulatory regions to influence
99 expression levels (Wittkopp and Kalay 2011; Signor and Nuzhdin 2018).

100 It is possible to use RNAseq to identify mechanisms of gene expression divergence
101 between parental species by bringing *cis* elements from both parents together in the same *trans*
102 environment in F1 hybrids and quantifying allele specific expression (ASE) of parental alleles at
103 heterozygous sites (Cowles et al. 2002; Wittkopp et al. 2004; Signor and Nuzhdin 2018).
104 Determining whether a candidate gene is differentially expressed due to *cis*- or *trans*-regulatory
105 divergence is important to identify putatively causal alleles that can be further validated by
106 genome editing or transgenesis experiments. Furthermore, this type of analysis can reveal the
107 relative contribution of *cis*- and *trans*- variation influencing genome-wide patterns of expression
108 divergence. Some studies have found a larger contribution of *cis*-regulatory variation underlying
109 expression divergence between species (Graze et al. 2009; Shi et al. 2012; Schaefer et al. 2013;
110 Davidson and Balakrishnan 2016; Mack and Nachman 2017), whereas others have shown
111 expression patterns dominated by *trans*-acting variation (Streisfeld and Rausher 2009; McManus
112 et al. 2010; Hart et al. 2018). Overall, *cis*-acting alleles are generally thought to contribute more
113 to interspecific divergence and show mostly additive inheritance, while *trans*-acting alleles are
114 often more pleiotropic, contribute more to intraspecific divergence, and show non-additive
115 inheritance (Prud'homme et al. 2007; Lemos et al. 2008; Signor and Nuzhdin 2018).

116 Here, we combine whole-genome resequencing, RNAseq, and F1 hybrid allele specific
117 expression analyses to identify regulatory mechanisms influencing rapidly evolving craniofacial
118 phenotypes within an adaptive radiation of *Cyprinodon* pupfishes on San Salvador Island,
119 Bahamas (Fig. 1). This sympatric radiation consists of a dietary generalist species (*C. variegatus*)
120 and two endemic specialist species adapted to novel trophic niches – a molluscivore (*C.*
121 *brontotheroides*) and a scale-eater (*C. desquamator*; (Martin and Wainwright 2013a)). Nearly all
122 forty-nine pupfish species in the genus *Cyprinodon* distributed across North America and the
123 Caribbean are dietary generalists with similar craniofacial morphology that is used for
124 consuming algae and small invertebrates (Fig. 1A (Martin and Wainwright 2011; Martin and
125 Wainwright 2013b)). The molluscivore evolved short, thick oral jaws stabilized by a nearly
126 immobile maxilla allowing it to specialize on hard-shelled prey including ostracods and
127 gastropods (Fig. 1B). This morphology results in a larger in-lever to out-lever ratio compared
128 with generalists, increasing mechanical advantage for strong biting (Hernandez et al. 2018). The
129 molluscivore is also characterized by a prominent maxillary anteriodorsal protrusion that may be
130 used as a wedge for extracting snails from their shells (Martin et al. 2017; St. John, et al. 2020a).
131 The scale-eater is a predator that evolved to bite scales and protein-rich mucus removed from
132 other pupfish species during rapid feeding strikes (Fig. 1C (St. John, et al. 2020b)). Scale-eaters
133 have greatly enlarged oral jaws, larger adductor mandibulae muscles, darker breeding coloration,
134 and a more elongated body compared with the generalist and molluscivore species (Martin and
135 Wainwright 2013a).

136 Exceptional craniofacial divergence despite extremely recent divergence times and low
137 genetic differentiation between molluscivores and scale-eaters make this system a compelling
138 evolutionary model for human craniofacial developmental disorders. These trophic specialist
139 species rapidly diverged from an ancestral generalist phenotype within the last 10-15k years
140 (Turner et al. 2008; Martin and Feinstein 2014). Molluscivores and scale-eaters readily hybridize
141 in the laboratory to produce fertile F1 offspring with approximately intermediate craniofacial
142 phenotypes between the parents and no obvious sex ratio distortion (Martin and Wainwright
143 2013b; Martin and Feinstein 2014). These species show evidence of pre-mating isolation in the
144 laboratory (West and Kodric-Brown 2015) and are genetically differentiated in sympatry
145 (genome-wide mean $Fst = 0.14$ across 12 million SNPs; (McGirr and Martin 2017)).

146 We previously identified 31 genomic regions (20 kb) that contained SNPs fixed between
147 species ($Fst = 1$), showed signs of a hard selective sweep, and were significantly associated with
148 oral jaw size using multiple genome-wide association mapping approaches (McGirr and Martin
149 2017). A subset of these fixed SNPs fell within significant QTL explaining 15% of variation in
150 oral jaw size and were near genes annotated for effects on skeletal system development (Martin
151 et al. 2017). Here we use complementary approaches to identify candidate causal variants
152 putatively influencing craniofacial divergence by 1) incorporating transcriptomic data from 122
153 individuals sampled at three developmental stages (McGirr and Martin 2018; McGirr and Martin
154 2019), 2) applying genome divergence scans to a much larger sample of whole genomes from
155 San Salvador Island and surrounding Caribbean outgroup populations (increasing $n = 37$ to 258)
156 aligned to a new high-quality *de novo* genome assembly (Richards et al. 2020), 3) identifying
157 structural variation fixed between species for the first time in this system, and 4) inferring *cis* and
158 *trans* regulatory mechanisms underlying gene expression divergence between species using 12
159 F1 hybrid transcriptomes. Overall, we found that *trans*-regulatory divergence was responsible for
160 more expression divergence between species than *cis*-regulatory mechanisms. We also identified
161 two genes showing *cis*-regulatory divergence that were near just one fixed variant each: a
162 deletion upstream of a gene known to influence skeletal development (*dync2li1*) and a SNP
163 downstream of a novel skeletal candidate gene (*pycr3*). Our results highlight the utility of using
164 these closely related species replicated across isolated lake populations as an evolutionary model
165 for craniofacial development and provide highly promising candidate variants for future
166 functional validation experiments.

167

168 **Results**

169 ***Few fixed variants between young species showing drastic craniofacial divergence***

170 We analyzed whole genome resequencing samples for 258 *Cyprinodon* pupfishes (median
171 coverage = 8 \times ; (Richards et al. 2020)). This included 114 individuals from multiple isolated lake
172 populations on San Salvador Island (33 generalists, 46 molluscivores, and 35 scale-eaters) and
173 140 outgroup generalist pupfishes from across the Caribbean and North America. Libraries for
174 150PE Illumina sequencing were generated from DNA extracted from muscle tissue and the
175 resulting reads were mapped to the *C. brontotheroides* reference genome (v 1.0; total sequence
176 length = 1,162,855,435 bp; number of scaffolds = 15,698, scaffold N50, = 32,000,000 bp; L50 =

177 15 scaffolds; (Richards et al. 2020)). Variants were called using the Genome Analysis Toolkit
178 (GATK v 3.5 (DePristo et al. 2011)) and filtered to include SNPs with a minor allele frequency
179 above 0.05, genotype quality above 20, and sites with greater than 50% genotyping rate across
180 all individuals.

181 Out of 9.3 million SNPs identified in our dataset, we found a mere 157 SNPs fixed
182 between molluscivore and scale-eater specialist species showing $Fst = 1$ (Fig. 2A; mean genome-
183 wide $Fst = 0.076$). Of these 157 variants, 46 were within 10 kb of 27 genes and none were in
184 coding regions. These 27 genes were enriched for 27 biological processes ($P < 0.05$), including
185 several ontologies describing neuronal development and activity of cell types within bone
186 marrow (Fig. 2B; Table S1).

187 Structural variants (including insertions, deletions, inversions, translocations, and copy
188 number variants) have been traditionally difficult to detect in non-model systems and ignored by
189 many early whole-genome comparative studies (Stapley et al. 2010; Ho et al. 2019;
190 Wellenreuther et al. 2019). We identified 80,012 structural variants across eight molluscivore
191 and scale-eater individuals using a method that calls variants based on combined evidence from
192 paired-end clustering and split read analysis (Rausch et al. 2012). Just 87 structural variants were
193 fixed between species and, strikingly, all structural variants were deletions fixed in scale-eaters.
194 This may reflect differences in the position of fitness optima between scale-eaters and
195 molluscivores relative to the putative ancestral optimum. We expect larger effect mutations, such
196 as deletions, to be more likely to fix in scale-eaters than molluscivores due to the more distant
197 position of the fitness optimum for scale-eating (Martin et al. 2017). Differences in population
198 size may also explain why all deletions are fixed in scale-eaters, which have a smaller effective
199 population size than molluscivores (Richards and Martin 2017; Richards et al. 2020). These
200 deletions ranged in size between 55 bp and 4,703 bp (Fig. 2C). Of these, 34 fixed deletions were
201 near 34 genes (Table S1). Only a single fixed deletion (1,256 bp) was found within a protein
202 coding region, spanning the entire fifth exon of *gpa33* (Fig. 3). The 34 genes near fixed deletions
203 were enriched for 36 biological processes ($P < 0.05$), including ontologies describing bone
204 development, mesenchyme development, fibroblast growth, and digestive tract development
205 (Fig. 2D).

206 Including SNPs and deletions, we found a total of 80 fixed variants within 10 kb of 59
207 genes (Table S1). Encouragingly, 41 of these genes (70%) also showed high between population

208 nucleotide divergence ($D_{xy} > 0.0083$ (genome-wide 90th percentile)), strengthening evidence for
209 adaptive divergence at these loci. Variants with larger effect sizes are predicted to fix faster than
210 variants with smaller effects. (Griswold 2006; Yeaman and Whitlock 2011; Stetter et al. 2018).
211 However, there are likely many alleles contributing to craniofacial divergence that are
212 segregating between populations of molluscivores and scale-eaters. We also identified genes near
213 SNPs showing lower values of F_{st} that were still highly differentiated between species ($F_{st} >$
214 0.72 (genome-wide 99th percentile) and $D_{xy} > 0.0083$ (genome-wide 90th percentile)) and within
215 20 kb of a gene. Using these thresholds, we found 63,542 SNPs near 1,940 genes. This gene set
216 was enriched for 420 biological processes ($P < 0.01$), including embryonic cranial skeleton
217 morphogenesis, bone mineralization, muscle structure development, and forebrain development
218 (Table S2).

219

220 ***Genes near fixed variants are differentially expressed throughout development***

221 All but one of the 80 variants fixed between species were in non-coding regions, suggesting that
222 these variants may affect species-specific phenotypes through regulation of nearby genes. In
223 order to identify patterns of gene expression divergence between species, we combined two
224 previous transcriptomic datasets spanning three developmental stages and three San Salvador
225 Island lake populations (McGirr and Martin 2018; McGirr and Martin 2019). F1 offspring were
226 sampled at 2 days post-fertilization (dpf), 8 dpf, and 20 dpf. RNA was extracted from whole
227 body tissue at 2 dpf and 8 dpf; whereas 20 dpf samples were dissected to only extract RNA from
228 craniofacial tissues (Table S3). The earlier developmental stages are described as stage 23 (2
229 dpf) and 34 (8 dpf) in a recent embryonic staging series of *C. variegatus* (Lencer and McCune
230 2018). The 2 dpf stage is comparable to the Early Pharyngula Period of zebrafish, when
231 multipotent neural crest cells have begun migrating to pharyngeal arches that will form the oral
232 jaws and most other craniofacial structures (Schilling and Kimmel 1994; Furutani-Seiki and
233 Wittbrodt 2004; Lencer et al. 2017). Embryos usually hatch six to ten days post fertilization, with
234 similar variation in hatch times among species (Lencer et al. 2017; McGirr and Martin 2018).
235 While some cranial elements are ossified prior to hatching, the skull is largely cartilaginous at 8
236 dpf and ossified by 20 dpf (Lencer and McCune 2018).

237 We used DEseq2 (Love et al. 2014) to contrast gene expression in pairwise comparisons
238 between species grouped by developmental stage (sample sizes for comparisons (molluscivores

239 vs. scale-eaters): 2 dpf = 6 vs. 6, 8 dpf = 8 vs. 10, 20 dpf = 6 vs. 2). Out of 19,304 genes
240 annotated for the *C. brontotheroides* reference genome, we found 770 (5.93%) significantly
241 differentially expressed at 2 dpf, 1,277 (9.48%) at 8 dpf, and 312 (2.50%) at 20 dpf (Fig. 4A-D).
242 The lower number of genes differentially expressed at 20 dpf likely reflects reduced power to
243 detect expression differences due to the small scale-eater sample size. Nonetheless, we found
244 four genes differentially expressed throughout development at all three stages (*filip1*, *c1galt1*,
245 *klhl24*, and *oit3*) and 248 genes were differentially expressed during two of the three stages
246 examined. Of the 59 genes within 10 kb of SNPs or deletions fixed between species, we found
247 12 differentially expressed during at least one developmental stage (Table 1; Fig. 4E). Two of
248 these genes (*dync2li1* and *pycr3*) were differentially expressed at 2 dpf and 8 dpf.

249 Since this is a young radiation, many other candidate adaptive loci are likely segregating
250 between species due to incomplete hard sweeps or because multiple adaptive haplotypes exist
251 causing signatures of soft sweeps. We also evaluated whether highly differentiated variants that
252 were not fixed between species may influence expression divergence. Of the 1,940 genes within
253 20 kb of highly differentiated SNPs ($Fst > 0.72$ and $Dxy > 0.0083$), 384 were differentially
254 expressed during at least one developmental stage (Fig. S1). This gene set was enriched for 87
255 biological processes, including pigment accumulation, vasculature development, lipid
256 localization, and regulation of keratinocyte differentiation ($P < 0.05$; Table S4 and S5).

257

258 ***Regulatory mechanisms underlying expression divergence between species***

259 Despite overall low genetic differentiation observed between species (genome-wide mean $Fst =$
260 0.076), we identified thousands of genes expressed in F1 hybrids containing heterozygous sites
261 that were alternately homozygous between parental populations (ranging between 18.5% –
262 28.5% of all genes expressed in F1 hybrids; Table S6). We measured allele specific expression
263 (ASE) for these genes using MBASED (Mayba et al. 2014) and inferred mechanisms of
264 regulatory divergence by comparing the ratio of maternal and paternal allelic expression in F1
265 hybrids with the ratio of molluscivore and scale-eater gene expression in purebred F1 offspring
266 (Fig. 5; (Cowles et al. 2002; Wittkopp et al. 2004; McManus et al. 2010; Mack et al. 2016)).

267 Most genes were expressed at a similar level in each species, as well as in F1 hybrids,
268 indicating conserved regulation (88.46% – 93.33%; Fig. 6). The majority of genes that were
269 differentially expressed between species showed *trans*-regulatory divergence (3.90% – 6.21%),

270 which accounted for more than three times the number of genes influenced by *cis*-regulatory
271 divergence (1.08% – 1.67%). *Trans*-regulatory divergence was also more prevalent than
272 expression influenced by a combination of *cis* and *trans* effects. The number of genes influenced
273 by *cis* × *trans* compensatory changes (0.80% – 2.25%) was similar to the number of genes
274 influenced by *cis* + *trans* reinforcing changes (0.76% – 2.01%).

275 *Cis*-regulatory variants are expected to contribute to additive inheritance of gene
276 expression in F1 hybrids, while *trans*-regulatory variants are expected to influence patterns of
277 dominance (Prud'homme et al. 2007; Lemos et al. 2008; Signor and Nuzhdin 2018).
278 Furthermore, *cis* × *trans* compensatory changes can result in transgressive gene expression,
279 where expression is significantly higher or lower in F1 hybrids compared to parental populations
280 (Landry et al. 2005; Landry et al. 2007; Mack and Nachman 2016; McGirr and Martin 2019).
281 We found additive, dominant, and transgressive patterns of gene expression inheritance in F1
282 hybrids at both developmental stages. Despite the overall lower contribution of *cis*-regulatory
283 divergence compared to *trans*-regulatory divergence, we found that slightly more genes showed
284 additive inheritance than dominant inheritance (Fig. S2; 2 dpf: additive = 4.49% dominant =
285 1.90%; 8 dpf: additive = 5.84% dominant = 3.85%).

286

287 ***Fixed variants near genes showing cis-regulatory divergence***

288 While most differential expression between species was explained by *trans*-regulatory
289 divergence, it is difficult to identify the down-stream targets of *trans*-acting alleles because they
290 are necessarily unlinked from the genes they regulate. Furthermore, it is unknown whether the
291 predominance of *trans*-regulatory divergence was driven by few alleles with numerous effects or
292 many alleles distributed throughout the genome. Thus, in order to identify candidate variation
293 causing differences in gene expression between molluscivores and scale-eaters, we examined
294 genes in highly differentiated regions of the genome that were differentially expressed due to *cis*-
295 regulatory divergence. We found a total of 148 genes showing *cis*-regulatory divergence among
296 all four F1 hybrid crosses (Fig. 6). We identified 37 of these genes (25%) within the set of 384
297 genes that were differentially expressed between species and within 20 kb of highly
298 differentiated SNPs ($Fst > 0.72$ and $D_{xy} > 0.0083$; Table S7).

299 We also found differentially expressed genes showing *cis*-regulatory divergence that
300 were near the most highly differentiated regions of the genome containing variants fixed between

301 species. Of the 12 genes that were within 10 kb of fixed variants, five contained heterozygous
302 sites that could be used to measure ASE (Fig. 7 and S3). Three of these (*eef1d*, *washc5*, and *pxk*)
303 showed *trans*-regulatory divergence (Fig. S3). The other two genes which were differentially
304 expressed at 2 dpf and 8 dpf (*sync2li1* and *pycr3*) showed *cis*-regulatory divergence (Fig. 7).
305 This provided strong evidence that differential regulation of these genes was influenced by
306 genetic divergence within putative *cis*-regulatory elements.

307 These two genes showing *cis*-regulatory divergence were near just one fixed variant each:
308 a 91 bp deletion located 7,384 bp upstream of *sync2li1* and an A-to-C transversion 1,808 bp
309 downstream of *pycr3* (Fig. 7). The next closest fixed variants were separated by greater than 600
310 kb and 31 kb, respectively. We searched the JASPAR database (Fornes et al. 2019) to identify
311 potential transcription factor binding sites that could be altered by these candidate *cis*-acting
312 variants. The 91 bp deletion near *sync2li1* contained binding motifs corresponding to seven
313 transcription factors (*nfia*, *nfia*, *nfic*, *znf384*, *hoxa5*, *gata1*, *myb*; Table S8). Two binding motifs
314 spanned the *pycr3* SNP region (*gata2*, *mzf1*), one of which, *mzf1*, was altered by the alternate
315 allele in scale-eaters. The scale-eater allele created a new potential binding motif matching the
316 transcription factor *plagl2*. Sanger sequencing confirmed the A-to-C transversion near *pycr3* in
317 four additional individuals not included in the whole-genome resequencing dataset (Fig. 8).

318

319 **Discussion**

320 Understanding the developmental genetic basis of complex traits by investigating natural
321 variation among closely related species is a powerful complementary approach to traditional
322 genetic screens in model systems. The San Salvador Island *Cyprinodon* pupfish system is a
323 useful evolutionary model for understanding the genetic basis of craniofacial defects and natural
324 diversity given extensive morphological divergence between these young species (Fig. 1). We
325 found thousands of genetic variants that were highly differentiated between molluscivore and
326 scale-eater species that were near genes that were differentially expressed at multiple
327 developmental stages. Just 244 variants were fixed between species across 9.3 million SNPs and
328 80,012 structural variants (Fig. 2A and C). Almost all fixed variants were in non-coding regions,
329 with the exception of an exon-spanning deletion (Fig. 3). In support of these variants affecting
330 divergent adaptive phenotypes, 80 variants were near 59 genes that were enriched for
331 developmental functions related to divergent specialist traits (Fig. 2B and D). Furthermore,

332 twelve of these genes were highly differentially expressed between species across three
333 developmental stages (Fig. 4E). By measuring allele-specific expression (ASE) in F1 hybrids
334 from multiple crosses between species, we found that *trans*-regulatory divergence explained
335 most patterns of expression divergence. We also identified two highly differentiated variants that
336 may act as *cis*-regulatory alleles affecting expression divergence between species: a fixed
337 deletion near *dync2l1* and a fixed SNP near *pycr3* (Fig. 7).

338

339 ***Gene regulatory divergence during rapid speciation***

340 Other studies investigating *cis* and *trans*-regulatory mechanisms have found that *cis*-acting
341 alleles contribute more to interspecific divergence, whereas *trans*-acting alleles contribute more
342 to intraspecific divergence (Prud'homme et al. 2007; Lemos et al. 2008; Signor and Nuzhdin
343 2018). Importantly, many of the studies supporting this pattern examine interspecific hybrids
344 generated by species pairs with much greater divergence times (Graze et al. 2009: *Drosophila*
345 *melanogaster* and *D. simulans* diverged 2.5 mya; Tirosh et al. 2009: *Saccharomyces cerevisiae*
346 and *S. paradoxus* diverged 5 mya; Shi et al. 2012: *Arabidopsis thaliana* and *A. arenosa* diverged
347 5.3 mya). Given that molluscivores and scale-eaters rapidly diverged within the past 10,000
348 years and are known to hybridize in the wild, we may see *trans*-effects dominating for the same
349 reasons *trans*-effects are thought to contribute more to intraspecific divergence. This is because,
350 both within species and between young species pairs, the larger mutational target of *trans*-
351 regulatory factors results in the observed excess of *trans*-effects (Wittkopp et al. 2008; Emerson
352 et al. 2010; Suvorov et al. 2013).

353 Similar to other studies, we found predominately additive patterns of gene inheritance in
354 F1 hybrids (Hughes et al. 2006; Rottscheidt and Harr 2007; Davidson and Balakrishnan 2016).
355 However, this contrasts with our finding of wide-spread *trans*-regulatory divergence, which is
356 expected to contribute to dominant and recessive patterns of inheritance (Lemos et al. 2008;
357 Signor and Nuzhdin 2018). Since genes were required to contain heterozygous sites in F1
358 hybrids for ASE analyses, we were only able to classify mechanisms of regulatory divergence
359 for a subset of genes used to classify modes of inheritance (Table S6). It is possible that
360 heterozygous genes were biased to show *trans*-regulatory divergence. It is also possible that we
361 underestimated the number of genes showing *cis*-regulatory divergence between species. We
362 required that genes show ASE across the entire coding region to assign *cis*-regulatory

363 divergence, which ignored the possibility of alleles affecting the expression of specific transcript
364 isoforms.

365

366 ***Fixed genetic variation influencing trophic specialization***

367 In a previous analysis of SNPs from a smaller whole genome dataset, *dync2li1* was one of 30
368 candidate genes that showed signs of a hard selective sweep and was significantly associated
369 with variation in jaw size between molluscivores and scale-eaters using multiple genome-wide
370 association mapping approaches (McGirr and Martin 2017). Here we show that a fixed deletion
371 near *dync2li1* may influence expression divergence between species through *cis*-acting
372 regulatory mechanisms. This gene (dynein cytoplasmic 2 light intermediate chain 1) is known to
373 influence skeletal morphology in humans (Kessler et al. 2015; Taylor et al. 2015; Niceta et al.
374 2018). It is a component of the cytoplasmic dynein 2 complex which is important for
375 intraflagellar transport – the movement of protein particles along the length of eukaryotic cilia
376 (Cole 2003; Pfister et al. 2006). Due to the vital role that cilia play in the transduction of signals
377 in the *hedgehog* pathway and other pathways important for skeletal development, disruptions in
378 dynein complexes cause a variety of skeletal dysplasias collectively termed skeletal ciliopathies
379 (Huber and Cormier-Daire 2012; Taylor et al. 2015). Mutations in *dync2li1* have been linked
380 with ciliopathies that result from abnormal cilia shape and function including Ellis-van Creveld
381 syndrome, Jeune syndrome, and short rib polydactyly syndrome (Kessler et al. 2015; Taylor et
382 al. 2015; Niceta et al. 2018). These disorders are characterized by variable craniofacial
383 malformations including micrognathia (small jaw), hypodontia (tooth absence), and cleft palate
384 (Brueton et al. 1990; Ruiz-Perez and Goodship 2009; Taylor et al. 2015). The discovery of
385 *dync2li1* as a candidate gene influencing differences in oral jaw length between molluscivores
386 and scale-eaters suggests that this system is particularly well-suited as an evolutionary mutant
387 model for clinical phenotypes involving jaw size, such as micrognathia and macrog纳thia.

388 We also identified a fixed SNP near the gene *pycr3* (pyrroline-5-carboxylate reductase 3;
389 also denoted *pycrl*) which showed *cis*-regulatory divergence. This gene is not currently known to
390 influence craniofacial phenotypes in humans or other model systems. However, one study
391 investigating gene expression divergence between beef and dairy breed bulls found that *pycr3*
392 was one of the most highly differentially expressed genes in skeletal muscle tissues. The authors
393 found nearly a three-fold difference in expression of *pycr3* between the two bull breeds that are

394 primarily characterized by differences in muscle anatomy (Sadkowski et al. 2009). Similarly,
395 expression changes in this gene may influence skeletal muscle development in specialists
396 species, which differ in the size of their adductor mandibulae muscles (Martin and Wainwright
397 2011; Hernandez et al. 2018). The A-to-C transversion near *pycr3* could influence differences in
398 expression by altering transcription factor binding. We found that the molluscivore allele
399 matches the binding motif of *mzf1* (myeloid zinc finger 1; Fig. 8), a transcription factor known to
400 influence cell proliferation (Gaboli et al. 2001), whereas the scale-eater allele alters this motif.
401 This type of binding motif analysis has a high sensitivity (*mzf1* is known to bind this motif) but
402 extremely low selectivity (*mzf1* does not bind nearly every occurrence of this motif, which
403 appears 1,430,540 times in the molluscivore reference genome).

404 While oral jaw size is the primary axis of phenotypic divergence in the San Salvador
405 Island pupfish system, adaptation to divergent niches required changes in a suite of
406 morphological and behavioral phenotypes (St John et al. 2019; St. John, Holzman, et al. 2020).
407 Most genes differentially expressed between species were found within whole embryo tissues
408 (Fig. 4A-D), suggesting we should find candidate genes influencing the development of
409 craniofacial phenotypes and other divergent traits. Of the 244 variants fixed between species, the
410 only coding variant was a 1,256 bp deletion that spanned the fifth exon of *gpa33* (glycoprotein
411 A33), which is expressed exclusively in intestinal epithelium (Fig. 3). Knockouts of this gene in
412 mice cause increased hypersensitivity to food allergens and susceptibility to a range of related
413 inflammatory intestinal pathologies (Williams et al. 2015). The gut contents of wild-caught
414 scale-eaters are comprised of 40-51% scales (Martin and Wainwright 2013c). The exon deletion
415 of *gpa33* may play a metabolic role in this unique adaptation that allows scale-eaters to occupy a
416 higher trophic level than molluscivores. Future studies in this system will benefit from
417 sequencing and analyses that target specific tissues and cell types to determine whether candidate
418 variants affect a single phenotype or have pleiotropic effects.

419

420 ***The effectiveness of Cyprinodon pupfishes for identifying candidate cis-regulatory variants***

421 One major advantage of investigating the genetic basis of craniofacial divergence between
422 molluscivores and scale-eaters is the low amount of genetic divergence between species.
423 Species-specific phenotypes are replicated across multiple isolated lake populations that exhibit
424 substantial ongoing gene flow. This has resulted in small regions of the genome showing strong

425 genetic differentiation (63,542 SNPs showing $Fst > 0.72$ and $Dxy > 0.0083$), with some regions
426 containing just a single variant fixed between species. The low number of fixed variants
427 dispersed across the genome makes this system relatively unique compared to other systems with
428 similar divergence times (Whiteley et al. 2010; Jones et al. 2012; Martin et al. 2019).

429 A previous study found a significant QTL explaining 15% of variation in oral jaw size
430 and three more potential moderate-effect QTL, suggesting that we may expect to find variants
431 with moderate effects on craniofacial divergence. Variants with larger effect sizes are predicted
432 to fix faster than variants with smaller effects, especially given short divergence times (Griswold
433 2006; Yeaman and Whitlock 2011; Stetter et al. 2018), which may suggest that the fixed variants
434 near *dync2li1* and *pycr3* have larger effects than segregating candidate alleles. However, these
435 fixed alleles are tightly linked with other highly differentiated alleles and may affect phenotypic
436 divergence through combined small effects with many closely clustered variants. Furthermore,
437 the fixation rate of mutations is not only dependent on effect size, but also dominance, which is
438 an important mode of gene expression inheritance in this system (Fig. S2) and other systems
439 (Gibson et al. 2004; Lemos et al. 2008; Signor and Nuzhdin 2018). While the fixed variants near
440 *dync2li1* and *pycr3* represent promising candidate alleles, adaptive differences in craniofacial
441 morphology are likely influenced by many loci, similar to polygenic traits studied in other
442 systems (Bergland et al. 2014; Boyle et al. 2017; Barghi et al. 2019; Sella et al. 2019).

443

444 **Conclusions**

445 Overall, our results highlight the utility of the San Salvador Island pupfish system as an
446 evolutionary mutant model for natural and clinical variation in human craniofacial phenotypes.
447 Similar rapid speciation replicated across many environments can be found in other adaptive
448 radiations (Martin et al. 2019; Martin and Richards 2019; Levin et al. 2020), which could also
449 prove useful as evolutionary models for a variety of other human traits. We found that a
450 combination of structural variant likely contribute to the evolution of highly divergent
451 craniofacial morphology, and that *trans*-regulatory mechanisms dominate patterns of expression
452 divergence between these young species. Future studies will attempt to validate the effect of
453 candidate variation on gene expression and craniofacial development *in vivo*.

454

455 **Methods**

456 ***Identifying genomic variation fixed between specialists***

457 In order to identify SNPs fixed between molluscivores and scale-eaters, we analyzed whole
458 genome resequencing samples for 258 individuals from across the Caribbean (median coverage =
459 8×; (Richards et al. 2020)). Briefly, 114 pupfishes from 15 isolated hypersaline lakes and one
460 estuary on San Salvador Island were collected using hand and seine nets between 2011 and 2018.
461 This included 33 generalists, 46 molluscivores, and 35 scale-eaters. Eight of these individuals
462 were bred to generate F1 offspring sampled for RNA sequencing (Table S3). This dataset also
463 included 140 outgroup generalist pupfishes from across the Caribbean and North America,
464 including two individuals belonging to the pupfish radiation in Lake Chichancanab, Mexico, and
465 two individuals from the most closely related outgroups to *Cyprinodon* (*Megupsilon aporus* and
466 *Cualac tessellatus* (Echelle et al. 2005)). Libraries for 150PE Illumina sequencing were
467 generated from DNA extracted from muscle tissue and the resulting reads were mapped to the *C.*
468 *brontotheroides* reference genome (v 1.0; total sequence length = 1,162,855,435 bp; number of
469 scaffolds = 15,698, scaffold N50, = 32,000,000 bp; L50 = 15 scaffolds; (Richards et al. 2020)).
470 Variants were called using the HaplotypeCaller function of the Genome Analysis Toolkit
471 (GATK v 3.5 (DePristo et al. 2011)). The GATK best practices workflow suggests using high-
472 quality known variants to act as a reference to recalibrate variant quality scores. Due to the lack
473 of a high confidence variant call set for this system, SNPs were filtered using conservative hard-
474 filtering parameters (Richards and Martin 2020; DePristo et al. 2011). SNPs were further filtered
475 to include SNPs with a minor allele frequency above 0.05, genotype quality above 20, and sites
476 with greater than 50% genotyping rate across all individuals, resulting in 9.3 million SNPs.

477 Measuring relative genetic differentiation (F_{ST}) between species can point to regions of
478 the genome containing variation affecting divergent phenotypes (Jones et al. 2012; Poelstra et al.
479 2014; Lamichhaney et al. 2015). However, F_{ST} is dependent on the many potential forces acting
480 to reduce within-population nucleotide diversity, including selective sweeps, purifying selection,
481 background selection, and low recombination rates (Noor and Bennett 2009; Cruickshank and
482 Hahn 2014). Measuring between-population divergence (D_{XY}) can help distinguish between
483 these possibilities because nucleotide divergence between species increases at loci under
484 different selective regimes (Nachman and Payseur 2012; Cruickshank and Hahn 2014; Irwin et
485 al. 2016). We measured F_{ST} between species with vcftools (v. 0.1.15; `weir-fst-pop` function) and
486 identified fixed SNPs ($F_{ST} = 1$). We also measured F_{ST} and D_{XY} in 10 kb and 20 kb windows

487 using the python script popGenWindows.py created by Simon Martin
488 (github.com/simonhmartin/genomics_general; (Martin et al. 2013)).

489 We identified structural variation (insertions, deletions, inversions, translocations, and
490 copy number variants) fixed between specialist species with DELLY (v 0.8.1; (Rausch et al.
491 2012)). Unlike GATK HaplotypeCaller which is limited to identifying structural variants smaller
492 than half the length of read size (DePristo et al. 2011), DELLY can identify small variants in
493 addition to variants larger than 300 bp using paired-end clustering and split read analysis. We
494 used DELLY to identify structural variants across eight whole genomes from the breeding pairs
495 used to generate F1 hybrid RNA samples (four scale-eaters from two lake populations and four
496 molluscivores from the same two lake populations; Table S3). First, we trimmed reads using
497 Trim Galore (v. 4.4, Babraham Bioinformatics), aligned them to the *C. brontotheroides* reference
498 genome with the Burrows-Wheeler Alignment Tool (v 0.7.12; (Li and Durbin 2011), and
499 removed duplicate reads from the resulting .bam files with Picard MarkDuplicates
500 (broadinstitute.github.io/picard). Second, we called variants with DELLY by comparing an
501 individual of one species with all individuals of the other species, resulting in eight variant call
502 files. Third, we identified structural variants fixed between species that were shared across all
503 eight files, in which all molluscivores showed the reference allele and all scale-eaters showed the
504 same alternate allele.

505

506 ***Transcriptomic sequencing, alignment, and variant discovery***

507 Our transcriptomic dataset included 50 libraries from 122 individuals sampled across three early
508 developmental stages (Table S3; (McGirr and Martin 2018; McGirr and Martin 2019)). Breeding
509 pairs used to generate F1 hybrids and purebred F1 offspring were collected from three
510 hypersaline lakes on San Salvador Island: Crescent Pond, Osprey Lake, and Little Lake. For
511 purebred crosses, we collected F1 embryos from breeding tanks containing multiple breeding
512 pairs from a single lake population. For F1 hybrid samples, we crossed a single individual of one
513 species with a single individual of another species from the same lake population.

514 RNA was extracted from samples collected two days after fertilization (2 dpf) eight days
515 after fertilization (8 dpf), and 17-20 days after fertilization (20 dpf) using RNeasy Mini Kits
516 (Qiagen catalog #74104). For samples collected at 2 dpf, we pooled 5 embryos together and
517 pulverized them in a 1.5 ml Eppendorf tube using a plastic pestle washed with RNase Away

518 (Molecular BioProducts). We used the same extraction method for samples collected at 8 dpf but
519 did not pool larvae and prepared a library for each individual separately. We dissected samples
520 collected at 20 dpf to isolate tissues from the anterior craniofacial region containing the dentary,
521 angular articular, maxilla, premaxilla, palatine, and associated craniofacial connective tissues
522 using fine-tipped tweezers washed with RNase AWAY. All samples were reared in breeding
523 tanks at 25–27°C, 10–15 ppt salinity, pH 8.3, and fed a mix of commercial pellet foods and
524 frozen foods.

525 Methods for total mRNA sequencing were previously described (McGirr and Martin
526 2018; McGirr and Martin 2019). Briefly, 2 dpf and 8 dpf libraries were prepared using TruSeq
527 stranded mRNA kits and sequenced on 3 lanes of Illumina 150 PE Hiseq4000 at the Vincent J.
528 Coates Genomic Sequencing Center (McGirr and Martin 2019). All 20 dpf libraries were
529 prepared using the KAPA stranded mRNA-seq kit at the High Throughput Genomic Sequencing
530 Facility at UNC Chapel Hill and sequenced on one lane of Illumina 150PE Hiseq4000 (McGirr
531 and Martin 2018). We filtered raw reads using Trim Galore (v. 4.4, Babraham Bioinformatics) to
532 remove Illumina adaptors and low-quality reads (mean Phred score < 20) and mapped
533 122,090,823 filtered reads to the *C. brontotheroides* reference genome (Richards et al. 2020)
534 using the RNAseq aligner STAR with default parameters (v. 2.5 (Dobin et al. 2013)). We
535 assessed mapping and read quality using MultiQC (Ewels et al. 2016) and quantified the number
536 of duplicate reads and the median percent GC content of mapped reads for each sample using
537 RSeQC (Wang et al. 2012). Although all reads were mapped to a molluscivore reference
538 genome, we did not find a significant difference between species in the proportion of reads
539 uniquely mapped with STAR (Fig. S4 A; Student's t-test, $P = 0.061$). Additionally, we did not
540 find a difference between species in the proportion of multimapped reads, GC content of reads,
541 or number of duplicate reads (Fig. S4 B-D; Student's t-test, $P > 0.05$).

542 We used GATK HaplotypeCaller function to call SNPs across 50 quality filtered
543 transcriptomes. We refined SNPs using the allele-specific software WASP (v. 0.3.3) to correct
544 for potential mapping biases that would influence tests of allele-specific expression (ASE; (Van
545 De Geijn et al. 2015)). WASP identified reads that overlapped SNPs in the initial .bam files and
546 re-mapped those reads after swapping the genotype for the alternate allele. Reads that failed to
547 map to exactly the same location were discarded. We re-mapped unbiased reads to create our

548 final .bam files used for differential expression analyses. Finally, we re-called SNPs using
549 unbiased .bam files for allele specific expression analyses.

550

551 ***Differential expression analyses***

552 We used the featureCounts function of the Rsubread package (Liao et al. 2014) requiring paired-
553 end and reverse stranded options to generate read counts across 19,304 genes and 156,743 exons
554 annotated for the molluscivore (*C. brontotheroides*) reference genome (Richards et al. 2020). We
555 used DESeq2 (v. 3.5 (Love et al. 2014)) to normalize raw read counts for library size and
556 perform principal component analyses, and identify differentially expressed genes. DESeq2 fits
557 negative binomial generalized linear models for each gene across samples to test the null
558 hypothesis that the fold change in gene expression between two groups is zero. Significant
559 differential expression between groups was determined with Wald tests by comparing
560 normalized posterior log fold change estimates and correcting for multiple testing using the
561 Benjamini–Hochberg procedure with a false discovery rate of 0.01 (Benjamini and Hochberg
562 1995).

563 We constructed a DESeqDataSet object in R using a multi-factor design that accounted
564 for variance in F1 read counts influenced by parental population origin and sequencing date
565 (design = ~sequencing_date + parental_breeding_pair_populations). Next, we used a variance
566 stabilizing transformation on normalized counts and performed a principal component analysis to
567 visualize the major axes of variation in 2 dpf, 8 dpf, and 20 dpf samples (Fig. S5). We contrasted
568 gene expression in pairwise comparisons between species grouped by developmental stage
569 (sample sizes for comparisons (molluscivores vs. scale-eaters): 2 dpf = 6 vs. 6, 8 dpf = 8 vs. 10,
570 20 dpf = 6 vs. 2).

571 We used pyranges (v. 1.6.5; (Lee et al. 2019)) to identify genetic variants overlapping
572 with gene regions. For each gene we identified variants within 10 kb of the start of the first exon
573 and within 10 kb of the end of the last exon). We also searched within 20 kb of genes, which is
574 the distance at which linkage disequilibrium decays to background levels (McGirr and Martin
575 2017). Using these window sizes, we were only able to identify differentiated regions of the
576 genome as candidate *cis*-regulatory regions that may influence expression levels of linked genes.
577 This approach does not take into account the action of distal regulatory regions acting at longer
578 ranges.

579

580 ***Allele specific expression analyses***

581 Our SNP dataset included every parent used to generate F1 hybrids between populations ($n = 8$).
582 We used the GATK VariantsToTable function (DePristo et al. 2011) to output genotypes across
583 9.3 million SNPs for each parent and overlapped these sites with the variant sites identified in F1
584 hybrid transcriptomes. We used python scripts (github.com/joemcgirr/fishfASE) to identify
585 SNPs that were alternatively homozygous in breeding pairs and heterozygous in their F1
586 offspring. We counted reads across heterozygous sites using ASEReadCounter (-minDepth 20 --
587 minMappingQuality 10 --minBaseQuality 20 -drf DuplicateRead) and matched read counts to
588 maternal and paternal alleles.

589 We identified significant allele-specific expression (ASE) using a beta-binomial test
590 comparing the maternal and paternal counts at each gene with the R package MBASED (Mayba
591 et al. 2014). For each F1 hybrid sample, we performed a 1-sample analysis with MBASED using
592 default parameters run for 1,000,000 simulations to determine whether genes showed significant
593 ASE in hybrids ($P < 0.05$). To test whether certain types of genes were disproportionately
594 included or excluded from ASE analyses due to the requirement that a gene contain heterozygous
595 sites in F1 hybrids, we determined how many of these genes were annotated for effects on
596 cranial skeletal system development (GO:1904888) and skeletal system development
597 (GO:0048705). We performed Fisher's exact tests for each cross, testing the null hypothesis that
598 the proportion of heterozygous genes within an ontology was equal to the proportion of non-
599 informative genes within an ontology. We did not find that genes involved in skeletal
600 development were disproportionately excluded from ASE analyses due to the requirement that a
601 gene contain heterozygous sites (Fisher's exact test, $P > 0.05$; Table S9).

602

603 ***Classifying regulatory mechanisms and inheritance in F1 hybrids***

604 It is possible to identify mechanisms of gene expression divergence between parental species by
605 bringing *cis* elements from both parents together in the same *trans* environment in F1 hybrids
606 and quantifying allele specific expression (ASE) of parental alleles at heterozygous sites (Fig. 5;
607 (Cowles et al. 2002; Wittkopp et al. 2004)). A gene that is differentially expressed between
608 parental species that also shows ASE biased toward one parental allele is expected to result from

609 *cis*-regulatory divergence. A gene that is differentially expressed between parental species that
610 does not show ASE in F1 hybrids is expected to result from *trans*-regulatory divergence.

611 In order to determine regulatory mechanisms controlling expression divergence between
612 parental species, a gene had to be included in differential expression analyses and ASE analyses.
613 We required that genes had at least two informative SNPs with $\geq 10\times$ coverage to assign
614 regulatory mechanisms. We calculated H – the ratio of maternal allele counts compared to the
615 number of paternal allele counts in F1 hybrids, and P – the ratio of normalized read counts in
616 purebred F1 offspring from the maternal population compared to read counts in purebred F1
617 offspring from the paternal population. We performed a Fisher’s exact test using H and P to
618 determine whether there was a significant *trans*- contribution to expression divergence (T),
619 testing the null hypothesis that the ratio of read counts in the parental populations was equal to
620 the ratio of parental allele counts in hybrids (Wittkopp et al. 2004; McManus et al. 2010;
621 Goncalves et al. 2012; Mack et al. 2016).

622 For each lake population at each developmental stage, we classified expression
623 divergence due to *cis*-regulation if a gene showed significant ASE in all F1 hybrids, significant
624 differential expression between parental populations of purebred F1 offspring, and no significant
625 T. We identified expression divergence due to *trans*-regulation if genes did not show ASE, were
626 differentially expressed between parental populations, and showed significant T. We defined *cis*
627 \times *trans* regulatory divergence if a gene showed H and P with opposing signs (*cis*- and *trans*-
628 regulatory factors had opposing effects on expression), significant ASE, significant T, and was
629 not differentially expressed between parental populations. We defined *cis* + *trans* regulatory
630 divergence if a gene showed H and P with the same sign (*cis*- and *trans*-regulatory factors had
631 the same effect on expression), significant ASE, significant T, and was not differentially
632 expressed between parental populations (McManus et al. 2010; Coolon et al. 2014; Mack et al.
633 2016).

634 For each developmental stage, we grouped species and F1 hybrids by lake population and
635 compared expression in F1 hybrids to expression in purebred offspring to determine whether
636 genes showed additive, dominant, or transgressive patterns of inheritance in hybrids. We
637 conducted four pairwise differential expression tests with DESeq2: 1) molluscivores vs. scale-
638 eaters 2) molluscivores vs. F1 hybrids 3) scale-eaters vs. F1 hybrids 4) molluscivores and scale-
639 eaters vs. F1 hybrids. Hybrid inheritance was considered additive if hybrid gene expression was

640 intermediate between parental populations and significantly different between parental
641 populations. Inheritance was dominant if hybrid expression was significantly different from one
642 parental population but not the other. Genes showing misexpression in hybrids showed
643 transgressive inheritance, meaning hybrid gene expression was significantly higher
644 (overdominant) or lower (underdominant) than both parental species.

645

646 ***Gene ontology enrichment and transcription factor binding site analyses***

647 We performed gene ontology (GO) enrichment analyses for genes near candidate adaptive
648 variants using ShinyGo v.0.51 (Ge et al. 2019). The *C. brontotheroides* reference genome was
649 annotated using MAKER, a genome annotation pipeline that annotates genes, transcripts, and
650 proteins (Cantarel et al. 2008). Gene symbols for orthologs identified by this pipeline largely
651 match human gene symbols. Thus, we searched for enrichment across biological process
652 ontologies curated for human gene functions.

653 We searched the JASPAR database (Fornes et al. 2019) to identify whether fixed
654 variation near genes showing *cis*-regulatory divergence altered potential transcription factor
655 binding sites. We generated fasta sequences for the molluscivore containing the variant site and
656 20 bp on either end of the site and searched across all 1011 predicted vertebrate binding motifs in
657 the database using a 95% relative profile score threshold. We then preformed the same analysis
658 for scale-eater fasta sequences containing the alternate allele.

659

660 ***Genotyping fixed variants***

661 In order to confirm the genotypes of putative *cis*-acting variants, we performed Sanger
662 sequencing on four additional individuals that were not included in our whole-genome dataset.
663 We extracted DNA from muscle tissue using DNeasy Blood and Tissue kits (Qiagen, Inc.) from
664 two molluscivores and two scale-eaters (wild samples were collected from Crescent Pond and
665 Osprey Lake for both species). We designed primers targeting the regions containing variation
666 fixed between species near the two genes showing evidence for *cis*-regulatory divergence (*pycr3*
667 and *dync2li1*) using the NCBI primer design tool (Ye et al. 2012). We designed primers targeting
668 a 446 bp region containing the SNP fixed between species (scaffold: HiC_scaffold_16 ; position:
669 1,0043,644) that was 1,808 bp downstream of *pycr3* (forward: 5'-
670 ACCATTCCAGAAGACAAAAAGCG-3'; reverse: 5'-GGCCCTATATGGGATGCACAA-

671 3'). Sequences were amplified with PCR using New England BioLabs *Taq* polymerase (no.
672 0141705) and dNTP solution (no. 0861609) and Sanger sequencing was performed at Eton
673 Bioscience Inc. (Research Triangle Park, North Carolina). Aligning the resulting sequences using
674 the Clustal Omega Multiple Sequence Alignment Tool (Madeira et al. 2019)) confirmed the A-
675 to-C transversion in scale-eaters (Fig. 8). We designed two additional primer sets targeting the
676 deletion region near *dync2li1* (scaffold: HiC_scaffold_43 ; position: 26,792,380-26,792,471).
677 While both primer sets amplified the sequence in molluscivore samples (not shown), we were
678 unable to amplify this region in scale-eaters, potentially due to high polymorphism in this region.
679

680 **Acknowledgements**

681 This study was funded by the University of North Carolina at Chapel Hill, the University of
682 California, Berkeley, NSF CAREER Award 1749764, and NIH/NIDCR R01 DE027052 to CHM
683 and a Graduate Research Fellowship from the Triangle Center for Evolutionary Medicine and an
684 SSE Rosemary Grant Travel Award to JAM. We thank Daniel Matute, Emilie Richards,
685 Michelle St. John, Bryan Reatini, and Sara Suzuki for valuable discussion; The Vincent J. Coates
686 Genomics Sequencing Laboratory at the University of California, Berkeley for performing RNA
687 library prep and Illumina sequencing; the Gerace Research Centre for logistics; and the
688 Bahamian government BEST Commission for permission to conduct this research.

689

690 **Competing Interests**

691 We declare no competing interests.

692

693 **Data Accessibility**

694 All transcriptomic raw sequence reads are available as zipped fastq files on the NCBI BioProject
695 database. Accession: PRJNA391309. Title: Craniofacial divergence in Caribbean Pupfishes. All
696 R and Python scripts used for pipelines are available on Github
697 (github.com/joemcgirr/fishfASE).

698

699 **Author Contributions**

700 JAM wrote the manuscript, extracted the RNA samples, and conducted all bioinformatic and
701 population genetic analyses. Both authors contributed to the conception and development of the
702 ideas and revision of the manuscript.

References

703 Ahi EP, Kapralova KH, Pálsson A, Maier VH, Gudbrandsson J, Snorrason SS, Jónsson ZO,
704 Franzdóttir SR. 2014. Transcriptional dynamics of a conserved gene expression network
705 associated with craniofacial divergence in Arctic charr. :1–19.

706 Albertson RC, Cresko W, Iii HWD, Postlethwait JH. 2008. Evolutionary mutant models for
707 human disease.

708 Albertson RC, Streelman JT, Kocher TD, Yelick PC. 2005. Integration and evolution of the
709 cichlid mandible : The molecular basis of alternate feeding strategies. 102:16287–16292.

710 Barghi N, Tobler R, Nolte V, Jakšić AM, Mallard F, Otte KA, Dolezal M, Taus T, Kofler R,
711 Schlötterer C. 2019. Genetic redundancy fuels polygenic adaptation in *Drosophila*.

712 Bergland AO, Behrman EL, O'Brien KR, Schmidt PS, Petrov DA. 2014. Genomic Evidence of
713 Rapid and Stable Adaptive Oscillations over Seasonal Time Scales in *Drosophila*. PLoS
714 Genet. 10.

715 Bono JM, Olesnický EC, Matzkin LM. 2015. Connecting genotypes, phenotypes and fitness:
716 Harnessing the power of CRISPR/Cas9 genome editing. Mol. Ecol. 24:3810–3822.

717 Boyle EA, Li YI, Pritchard JK. 2017. An Expanded View of Complex Traits: From Polygenic to
718 Omnipotent. Cell [Internet] 169:1177–1186. Available from:
719 <http://dx.doi.org/10.1016/j.cell.2017.05.038>

720 Brian K. Hall. 2009. The Neural Crest and Neural Crest Cells in Vertebrate Development and
721 Evolution. New York: Springer US

722 Brueton LA, Dillon MJ, Winter RM. 1990. Ellis-van Creveld syndrome, Jeune Syndrome, and

723 renal-hepatic-pancreatic dysplasia: Separate entities or disease spectrum? *J. Med. Genet.*
724 27:252–255.

725 Cantarel BL, Korf I, Robb SMC, Parra G, Ross E, Moore B, Holt C, Alvarado AS, Yandell M.
726 2008. MAKER: An easy-to-use annotation pipeline designed for emerging model organism
727 genomes. *Genome Res.* 18:188–196.

728 Cleves PA, Ellis NA, Jimenez MT, Nunez SM, Schluter D, Kingsley DM, Miller CT. 2014.
729 Evolved tooth gain in sticklebacks is associated with a cis-regulatory allele of *Bmp6*. *Proc.*
730 *Natl. Acad. Sci. [Internet]* 111:13912–13917. Available from:
731 <http://www.pnas.org/content/111/38/13912>

732 Cole DG. 2003. The intraflagellar transport machinery of *Chlamydomonas reinhardtii*. *Traffic*
733 4:435–442.

734 Conway JR, Lex A, Gehlenborg N. 2017. UpSetR: An R package for the visualization of
735 intersecting sets and their properties. *Bioinformatics* 33:2938–2940.

736 Coolon JD, Mcmanus CJ, Stevenson KR, Coolon JD, Mcmanus CJ, Stevenson KR, Graveley
737 BR, Wittkopp PJ. 2014. Tempo and mode of regulatory evolution in *Drosophila* Tempo and
738 mode of regulatory evolution in *Drosophila*. :797–808.

739 Cowles CR, Hirschhorn JN, Altshuler D, Lander ES. 2002. Detection of regulatory variation in
740 mouse genes. *Nat. Genet.* 32:432–437.

741 Cruickshank TE, Hahn MW. 2014. Reanalysis suggests that genomic islands of speciation are
742 due to reduced diversity, not reduced gene flow. *Mol. Ecol.* 23:3133–3157.

743 Davidson JH, Balakrishnan CN. 2016. Gene Regulatory Evolution During Speciation in a
744 Songbird. 6:1357–1364.

745 DePristo MA, Banks E, Poplin R, Garimella K V, Maguire JR, Hartl C, Philippakis AA, del
746 Angel G, Rivas MA, Hanna M, et al. 2011. A framework for variation discovery and
747 genotyping using next-generation DNA sequencing data. *Nat. Genet. [Internet]* 43:491–498.
748 Available from:
749 <http://www.pubmedcentral.nih.gov/articlerender.fcgi?artid=3083463&tool=pmcentrez&rendertype=abstract>

751 Dobin A, Davis CA, Schlesinger F, Drenkow J, Zaleski C, Jha S, Batut P, Chaisson M, Gingeras
752 TR. 2013. STAR: Ultrafast universal RNA-seq aligner. *Bioinformatics* 29:15–21.

753 Echelle AA, Carson EW, Echelle AF, Van Den Bussche RA, Dowling TE, Meyer A. 2005.

754 Historical Biogeography of the New-World Pupfish Genus *Cyprinodon* (Teleostei:
755 *Cyprinodontidae*). *Copeia* 2005:320–339.

756 Erickson PA, Baek J, Hart JC, Cleves PA, Miller CT. 2018. Genetic dissection of a supergene
757 implicates *tfap2a* in craniofacial evolution of threespine sticklebacks. *Genetics* 209:591–
758 605.

759 Ewels P, Lundin S, Max K. 2016. Data and text mining MultiQC : summarize analysis results for
760 multiple tools and samples in a single report. *32*:3047–3048.

761 Fornes O, Castro-Mondragon JA, Khan A, van der Lee R, Zhang X, Richmond PA, Modi BP,
762 Correard S, Gheorghe M, Baranašić D, et al. 2019. JASPAR 2020: update of the open-
763 access database of transcription factor binding profiles. *Nucleic Acids Res.* [Internet]:1–6.
764 Available from:
765 http://fdslive.oup.com/www.oup.com/pdf/production_in_progress.pdf%0Ahttp://www.ncbi.nlm.nih.gov/pubmed/31701148

766 Furutani-Seiki M, Wittbrodt J. 2004. Medaka and zebrafish, an evolutionary twin study. *Mech.
767 Dev.* 121:629–637.

768 Gaboli M, Kotsi PA, Gurrieri C, Cattoretti G, Ronchetti S, Cordon-Cardo C, Broxmeyer HE,
769 Hromas R, Pandolfi PP. 2001. *Mzf1* controls cell proliferation and tumorigenesis. *Genes
770 Dev.* 15:1625–1630.

771 Ge SX, Jung D, Yao R. 2019. ShinyGO: a graphical gene-set enrichment tool for animals and
772 plants. *Bioinformatics*:1–2.

773 Van De Geijn B, McVicker G, Gilad Y, Pritchard JK. 2015. WASP: Allele-specific software for
774 robust molecular quantitative trait locus discovery. *Nat. Methods* 12:1061–1063.

775 Gibson G, Riley-Berger R, Harshman L, Kopp A, Vacha S, Nuzhdin S, Wayne M. 2004.
776 Extensive sex-specific nonadditivity of gene expression in *Drosophila melanogaster*.
777 *Genetics* 167:1791–1799.

778 Goncalves A, Leigh-Brown S, Thybert D, Stefflova K, Turro E, Flicek P, Brazma A, Odom DT,
779 Marioni JC. 2012. Extensive compensatory *cis-trans* regulation in the evolution of mouse
780 gene expression. *Genome Res.* [Internet] 22:2376–2384. Available from:
781 <http://www.ncbi.nlm.nih.gov/pmc/articles/PMC3514667/>
782 <http://www.ncbi.nlm.nih.gov/pubmed/22919075>
783 <http://www.ncbi.nlm.nih.gov/genome/cshlp.org/content/22/12/2376.long>

785 Gorlin RJ, Cohen MM, Hennekam R. 1990. *Syndromes of the head and neck*. Oxford, UK:
786 Oxford University Press

787 Graze RM, McIntyre LM, Main BJ, Wayne ML, Nuzhdin S V. 2009. Regulatory divergence in
788 *Drosophila melanogaster* and *D. simulans*, a genomewide analysis of allele-specific
789 expression. *Genetics* 183:547–561.

790 Griswold CK. 2006. Gene flow's effect on the genetic architecture of a local adaptation and its
791 consequences for QTL analyses. *Heredity (Edinb)*. [Internet] 96:445–453. Available from:
792 <http://www.nature.com.proxy2.cl.msu.edu/hdy/journal/v96/n6/full/6800822a.html%5Cnhttp://www.nature.com.proxy2.cl.msu.edu/hdy/journal/v96/n6/pdf/6800822a.pdf>

793 Gross JB, Powers AK. 2018. A Natural Animal Model System of Craniofacial Anomalies: The
794 Blind Mexican Cavefish. *Anat. Rec.*

795 Hart JC, Ellis NA, Eisen MB, Miller CT. 2018. Convergent evolution of gene expression in two
796 high-toothed stickleback populations. *PLoS Genet.* 14:1–22.

797 Helms JA, Cordero D, Tapadia MD. 2005. New insights into craniofacial morphogenesis.
798 *Development* 132:851–861.

799 Hernandez LP, Adriaens D, Martin CH, Wainwright PC, Masschaele B, Dierick M. 2018.
800 Building trophic specializations that result in substantial niche partitioning within a young
801 adaptive radiation. *J. Anat.* 232:173–185.

802 Hindorff LA, Sethupathy P, Junkins HA, Ramos EM, Mehta JP, Collins FS, Manolio TA. 2009.
803 Potential etiologic and functional implications of genome-wide association loci for human
804 diseases and traits. *Proc. Natl. Acad. Sci. U. S. A.* 106:9362–9367.

805 Ho SS, Urban AE, Mills RE. 2019. Structural variation in the sequencing era. *Nat. Rev. Genet.*
806 [Internet]. Available from: <http://www.ncbi.nlm.nih.gov/pubmed/31729472>

807 Huber C, Cormier-Daire V. 2012. Ciliary disorder of the skeleton. *Am. J. Med. Genet. Part C*
808 *Semin. Med. Genet.* 160 C:165–174.

809 Irwin DE, Alcaide M, Delmore KE, Irwin JH, Owens GL. 2016. Recurrent selection explains
810 parallel evolution of genomic regions of high relative but low absolute differentiation in a
811 ring species. *Mol. Ecol.* 25:4488–4507.

812 St. John ME, Dixon KE, Martin CH. 2020. Oral shelling within an adaptive radiation of
813 pupfishes: Testing the adaptive function of a novel nasal protrusion and behavioural
814 preference. *J. Fish Biol.*:1–9.

815

816 St. John ME, Holzman R, Martin CH. 2020. Rapid adaptive evolution of scale-eating kinematics
817 to a novel ecological niche. *J. Exp. Biol.*:jeb.217570.

818 Jones FC, Grabherr MG, Chan YF, Russell P, Mauceli E, Johnson J, Swofford R, Pirun M, Zody
819 MC, White S, et al. 2012. The genomic basis of adaptive evolution in threespine
820 sticklebacks. *Nature*.

821 Kessler K, Wunderlich I, Uebe S, Falk NS, Gießl A, Helmut Brandstätter J, Popp B, Klinger P,
822 Ekici AB, Sticht H, et al. 2015. DYNC2LI1 mutations broaden the clinical spectrum of
823 dynein-2 defects. *Sci. Rep.* 5:1–12.

824 Kratochwil CF, Meyer A. 2015. Closing the genotype-phenotype gap: Emerging technologies for
825 evolutionary genetics in ecological model vertebrate systems. *BioEssays* 37:213–226.

826 Lamichhaney S, Berglund J, Almén MS, Maqbool K, Grabherr M, Martinez-Barrio A,
827 Promerová M, Rubin C-J, Wang C, Zamani N, et al. 2015. Evolution of Darwin's finches
828 and their beaks revealed by genome sequencing. *Nature* [Internet] 518:371–375. Available
829 from: <http://www.nature.com/doifinder/10.1038/nature14181>

830 Landry CR, Hartl DL, Ranz JM. 2007. Genome clashes in hybrids: Insights from gene
831 expression. *Heredity (Edinb)*. 99:483–493.

832 Landry CR, Wittkopp PJ, Taubes CH, Ranz JM, Clark AG, Hartl DL. 2005. Compensatory cis-
833 trans evolution and the dysregulation of gene expression in interspecific hybrids of
834 *drosophila*. *Genetics* 171:1813–1822.

835 Lee S, Cook D, Lawrence M. 2019. Plyranges: A grammar of genomic data transformation.
836 *Genome Biol.* 20:1–10.

837 Lemos B, Araripe LO, Fontanillas P, Hartl DL. 2008. Dominance and the evolutionary
838 accumulation of cis- and trans-effects on gene expression. *Proc. Natl. Acad. Sci.* [Internet]
839 105:14471–14476. Available from: <http://www.pnas.org/cgi/doi/10.1073/pnas.0805160105>

840 Lencer ES, McCune AR. 2018. An embryonic staging series up to hatching for *Cyprinodon*
841 *variegatus*: An emerging fish model for developmental, evolutionary, and ecological
842 research. *J. Morphol.* 279:1559–1578.

843 Lencer ES, Warren WC, Harrison R, McCune AR. 2017. The *Cyprinodon variegatus* genome
844 reveals gene expression changes underlying differences in skull morphology among closely
845 related species. :1–33.

846 Levin BA, Simonov E, Dgebuadze YY, Levina M, Golubtsov AS. 2020. In the rivers: Multiple

847 adaptive radiations of cyprinid fishes (*Labeobarbus*) in Ethiopian Highlands. *Sci. Rep.*
848 10:1–13.

849 Li H, Durbin R. 2011. Inference of human population history from individual whole-genome
850 sequences. *Nature* [Internet] 475:493–496. Available from:
851 <http://dx.doi.org/10.1038/nature10231>

852 Liao Y, Smyth GK, Shi W. 2014. Sequence analysis featureCounts : an efficient general purpose
853 program for assigning sequence reads to genomic features. 30:923–930.

854 Love MI, Huber W, Anders S. 2014. Moderated estimation of fold change and dispersion for
855 RNA-seq data with DESeq2. :1–21.

856 Mack KL, Campbell P, Nachman MW. 2016. Gene regulation and speciation in house mice.
857 :451–461.

858 Mack KL, Nachman MW. 2017. Gene Regulation and Speciation. *Trends Genet.* 33:68–80.

859 Madeira F, Park YM, Lee J, Buso N, Gur T, Madhusoodanan N, Basutkar P, Tivey ARN, Potter
860 SC, Finn RD, et al. 2019. The EMBL-EBI search and sequence analysis tools APIs in 2019.
861 *Nucleic Acids Res.* 47:W636–W641.

862 Martin CH, Erickson PA, Miller CT. 2017. The genetic architecture of novel trophic specialists:
863 larger effect sizes are associated with exceptional oral jaw diversification in a pupfish
864 adaptive radiation. *Mol. Ecol.* 26:624–638.

865 Martin CH, Feinstein LC. 2014. Novel trophic niches drive variable progress towards ecological
866 speciation within an adaptive radiation of pupfishes. *Mol. Ecol.* 23:1846–1862.

867 Martin Christopher H, McGirr JA, Richards EJ, St. John M. 2019. How to investigate the origins
868 of novelty: insights gained from genetic, behavioral, and fitness perspectives. *Integr. Org.*
869 *Biol.*

870 Martin C H, McGirr JA, Richards EJ, St. John ME. 2019. How to Investigate the Origins of
871 Novelty: Insights Gained from Genetic, Behavioral, and Fitness Perspectives. *Integr. Org.*
872 *Biol.* 1.

873 Martin CH, Richards EJ. 2019. The Paradox Behind the Pattern of Rapid Adaptive Radiation:
874 How Can the Speciation Process Sustain Itself Through an Early Burst? *Annu. Rev. Ecol.*
875 *Evol. Syst.* 50:1–25.

876 Martin CH, Wainwright PC. 2011. Trophic novelty is linked to exceptional rates of
877 morphological diversification in two adaptive radiations of *Cyprinodon* pupfish. *Evolution*

878 [Internet] 65:2197–2212. Available from: <http://www.ncbi.nlm.nih.gov/pubmed/21790569>

879 Martin CH, Wainwright PC. 2013a. A remarkable species flock of Cyprinodon pupfishes

880 endemic to San Salvador Island, Bahamas. *Bull. Peabody Museum Nat. Hist.* [Internet]

881 54:231–241. Available from: file:///Users/antoniaford/Library/Application

882 Support/Papers2/Articles/2013/Martin/Martin_Bulletin_of_the_Peabody_Museum_of_Natu

883 ral_History_2013-1.pdf%5Cn<http://www.bioone.org/doi/abs/10.3374/014.054.0201>

884 Martin CH, Wainwright PC. 2013b. Multiple fitness peaks on the adaptive landscape drive

885 adaptive radiation in the wild. *Science* [Internet] 339:208–211. Available from:

886 <http://science.sciencemag.org/content/339/6116/208.abstract>

887 Martin CH, Wainwright PC. 2013c. On the measurement of ecological novelty: scale-eating

888 pupfish are separated by 168 my from other scale-eating fishes. *PLoS One* [Internet]

889 8:e71164. Available from:

890 <http://www.ncbi.nlm.nih.gov/pmc/articles/PMC3747246/>&tool=pmcentrez&rendertype=abstract

891

892 Martin SH, Dasmahapatra KK, Nadeau NJ, Salazar C, Walters JR, Simpson F, Blaxter M,

893 Manica A, Mallet J, Jiggins CD. 2013. Genome-wide evidence for speciation with gene

894 flow in *Heliconius* butterflies. *Genome Res.* 23:1817–1828.

895 Maurano MT, Humbert R, Rynes E, Thurman RE, Haugen E, Wang H, Reynolds AP, Sandstrom

896 R, Qu H, Brody J, et al. 2012. Systematic localization of common disease-associated

897 variation in regulatory DNA. *Science* (80-.). 337:1190–1195.

898 Mayba O, Gilbert HN, Liu J, Haverty PM, Jhunjhunwala S, Jiang Z, Watanabe C, Zhang Z.

899 2014. MBASED: Allele-specific expression detection in cancer tissues and cell lines.

900 *Genome Biol.* 15:1–21.

901 McGirr J, Martin C. 2019. Ecological divergence in sympatry causes gene misregulation in

902 hybrids. *bioRxiv* 717025:1–71.

903 McGirr JA, Martin CH. 2017. Novel candidate genes underlying extreme trophic specialization

904 in caribbean pupfishes. *Mol. Biol. Evol.* 34:873–888.

905 McGirr JA, Martin CH. 2018. Parallel evolution of gene expression between trophic specialists

906 despite divergent genotypes and morphologies. *Evol. Lett.* [Internet]:62–75. Available

907 from: <http://doi.wiley.com/10.1002/evl3.41>

908 McManus CJ, Coolon JD, Duff MO, Eipper-Mains J, Graveley BR, Wittkopp PJ. 2010.

909 Regulatory divergence in *Drosophila* revealed by mRNA-seq. *Genome Res.* 20:816–825.

910 Nachman MW, Payseur BA. 2012. Recombination rate variation and speciation: theoretical
911 predictions and empirical results from rabbits and mice. *Philos. Trans. R. Soc. B Biol. Sci.*
912 [Internet] 367:409–421. Available from:
913 <http://rstb.royalsocietypublishing.org/cgi/doi/10.1098/rstb.2011.0249>

914 Nguyen D, Tian X. 2008. The expanding role of mouse genetics for understanding human
915 biology and disease. *DMM Dis. Model. Mech.* 1:56–66.

916 Niceta M, Margiotti K, Digilio MC, Guida V, Bruselles A, Pizzi S, Ferraris A, Memo L,
917 Laforgia N, Dentici ML, et al. 2018. Biallelic mutations in DYNC2LI1 are a rare cause of
918 Ellis-van Creveld syndrome. *Clin. Genet.* 93:632–639.

919 Pfister KK, Shah PR, Hummerich H, Russ A, Cotton J, Annuar AA, King SM, Fisher EMC.
920 2006. Genetic analysis of the cytoplasmic dynein subunit families. *PLoS Genet.* 2:11–26.

921 Poelstra JW, Vijay N, Bossu CM, Lantz H, Ryll B, Müller I, Baglione V, Unneberg P, Wikelski
922 M, Grabherr MG, et al. 2014. The genomic landscape underlying phenotypic integrity in the
923 face of gene flow in crows. *Science* [Internet] 344:1410–1414. Available from:
924 <http://science.sciencemag.org/content/344/6190/1410.abstract>

925 Powder KE, Albertson RC. 2016. Cichlid fishes as a model to understand normal and clinical
926 craniofacial variation. *Dev. Biol.* [Internet] 415:338–346. Available from:
927 <http://dx.doi.org/10.1016/j.ydbio.2015.12.018>

928 Prud'homme B, Gompel N, Carroll SB. 2007. Emerging principles of regulatory evolution. *Proc.*
929 *Natl. Acad. Sci.* [Internet] 104:8605–8612. Available from:
930 <http://www.pnas.org/cgi/doi/10.1073/pnas.0700488104>

931 Rausch T, Zichner T, Schlattl A, Stütz AM, Benes V, Korbel JO. 2012. DELLY : structural
932 variant discovery by integrated paired-end and split-read analysis. 28:333–339.

933 Richards AEJ, McGirr JA, Wang JR, John MES. 2020. Major stages of vertebrate adaptive
934 radiation are assembled from a disparate spatiotemporal landscape.

935 Roberts RB, Hu Y, Albertson RC, Kocher TD. 2011. Craniofacial divergence and ongoing
936 adaptation via the hedgehog pathway. *Proc. Natl. Acad. Sci. U. S. A.* 108:13194–13199.

937 Ruiz-Perez VL, Goodship JA. 2009. Ellis-van Creveld syndrome and Weyers acrodermal
938 dysostosis are caused by cilia-mediated diminished response to Hedgehog ligands. *Am. J.*
939 *Med. Genet. Part C Semin. Med. Genet.* 151:341–351.

940 Sadkowski T, Jank M, Zwierzchowski L, Oprzadek J, Motyl T. 2009. Comparison of skeletal
941 muscle transcriptional profiles in dairy and beef breeds bulls. *J. Appl. Genet.* 50:109–123.

942 Schaefer B, Emerson JJ, Wang TY, Lu MYJ, Hsieh LC, Li WH. 2013. Inheritance of gene
943 expression level and selective constraints on trans-and cis-regulatory changes in yeast. *Mol.*
944 *Biol. Evol.* 30:2121–2133.

945 Schartl M. 2014. Beyond the zebrafish: Diverse fish species for modeling human disease. *DMM*
946 *Dis. Model. Mech.* 7:181–192.

947 Schaub MA, Boyle AP, Kundaje A, Batzoglou S, Snyder M. 2012. Linking disease associations
948 with regulatory information in the human genome. *Genome Res.* 22:1748–1759.

949 Schilling TF, Kimmel CB. 1994. Segment and cell type lineage restrictions during pharyngeal
950 arch development in the zebrafish embryo. *Development* [Internet] 120:483–494. Available
951 from: <http://www.ncbi.nlm.nih.gov/pubmed/8162849>

952 Sella Ggch, Sella Guy, Barton NH. 2019. Thinking About the Evolution of Complex Traits in the
953 Era of Genome-Wide Association Studies. :1–33.

954 Shi X, Ng DWK, Zhang C, Comai L, Ye W, Jeffrey Chen Z. 2012. Cis- and trans-regulatory
955 divergence between progenitor species determines gene-expression novelty in *Arabidopsis*
956 allopolyploids. *Nat. Commun.* [Internet] 3:950–959. Available from:
957 <http://dx.doi.org/10.1038/ncomms1954>

958 Signor SA, Nuzhdin S V. 2018. The Evolution of Gene Expression in cis and trans. *Trends*
959 *Genet.* [Internet]:1–13. Available from:
960 <http://linkinghub.elsevier.com/retrieve/pii/S0168952518300623>

961 St John ME, McGirr JA, Martin CH. 2019. The behavioral origins of novelty: Did increased
962 aggression lead to scale-eating in pupfishes? *Behav. Ecol.* 30:557–569.

963 Stapley J, Reger J, Feulner PGD, Smadja C, Galindo J, Ekblom R, Bennison C, Ball AD,
964 Beckerman AP, Slate J. 2010. Adaptation genomics: The next generation. *Trends Ecol.*
965 *Evol.* [Internet] 25:705–712. Available from: <http://dx.doi.org/10.1016/j.tree.2010.09.002>

966 Stetter MG, Thornton K, Ross-Ibarra J. 2018. Genetic architecture and selective sweeps after
967 polygenic adaptation to distant trait optima. *PLoS Genet.* 14:1–24.

968 Streisfeld MA, Rausher MD. 2009. Altered trans-regulatory control of gene expression in
969 multiple anthocyanin genes contributes to adaptive flower color evolution in *Mimulus*
970 *aurantiacus*. *Mol. Biol. Evol.* 26:433–444.

971 Taylor SP, Dantas TJ, Duran I, Wu S, Lachman RS, Consortium G, Nelson SF, Cohn DH, Vallee
972 RB, Krakow D. 2015. and cause short rib polydactyly syndrome. *Nat. Commun.* [Internet]
973 6:1–11. Available from: <http://dx.doi.org/10.1038/ncomms8092>

974 Turner BJ, Duvernall DD, Bunt TM, Barton MG. 2008. Reproductive isolation among endemic
975 pupfishes (*Cyprinodon*) on San Salvador Island, Bahamas: Microsatellite evidence. *Biol. J.
976 Linn. Soc.* 95:566–582.

977 Verta JP, Jones FC. 2019. Predominance of cis-regulatory changes in parallel expression
978 divergence of sticklebacks. *Elife* 8:1–30.

979 Wang L, Wang S, Li W. 2012. RSeQC: quality control of RNA-seq experiments. *Bioinforma.
980 Oxford Engl.*

981 Wellenreuther M, Mérot C, Berdan E, Bernatchez L. 2019. Going beyond SNPs: The role of
982 structural genomic variants in adaptive evolution and species diversification. *Mol. Ecol.*
983 28:1203–1209.

984 West RJD, Kodric-Brown A. 2015. Mate Choice by Both Sexes Maintains Reproductive
985 Isolation in a Species Flock of Pupfish (*Cyprinodon* spp) in the Bahamas. *Ethology*
986 121:793–800.

987 Whiteley AR, Rogers SM, Derome N, Renaut S, Jeukens J, Bernatchez L, Nolte AW, Østbye K,
988 St-Cyr J, Lu G, et al. 2010. On the origin of species: insights from the ecological genomics
989 of lake whitefish. *Philos. Trans. R. Soc. B Biol. Sci.* 365:1783–1800.

990 Williams BB, Tebbutt NC, Buchert M, Putoczki TL, Doggett K, Bao S, Johnstone CN, Masson
991 F, Hollande F, Burgess AW, et al. 2015. Glycoprotein A33 deficiency: A new mouse model
992 of impaired intestinal epithelial barrier function and inflammatory disease. *DMM Dis.
993 Model. Mech.* 8:805–815.

994 Wittkopp PJ, Haerum BK, Clark AG. 2004. Evolutionary changes in cis and trans gene
995 regulation. *Nature*.

996 Wittkopp PJ, Kalay G. 2011. Cis -regulatory elements : molecular mechanisms and evolutionary
997 processes underlying divergence. *Nat. Rev. Genet.* [Internet] 13:59–69. Available from:
998 <http://dx.doi.org/10.1038/nrg3095>

999 Ye J, Coulouris G, Zaretskaya I, Cutcutache I, Rozen S, Madden TL. 2012. Primer-BLAST: A
1000 tool to design target-specific primers for polymerase chain reaction.

1001 Yeaman S, Whitlock MC. 2011. The genetic architecture of adaptation under migration-selection

Table 1. Twelve genes differentially expressed between molluscivores and scale-eaters at 2 days post fertilization (dpf), 8 dpf, and/or 20 dpf ($P < 0.01$ in bold). MNC = mean normalized counts across all samples. LFC = log2 fold change in expression (positive values indicate higher expression in scale-eaters than molluscivores). P = adjusted P -value for differential expression (DESeq2).

gene	2 dpf			8 dpf			20 dpf		
	MNC	LFC	P	MNC	LFC	P	MNC	LFC	P
<i>dync2li1</i>	96.09	-0.70	3.7E-05	34.05	-1.05	5.2E-05	23.83	-1.10	1.2E-01
<i>pycr3</i>	221.91	0.49	2.5E-03	56.19	1.09	1.5E-08	38.16	0.13	8.9E-01
<i>eef1d</i>	1984.23	0.18	1.3E-01	1076.82	0.51	8.8E-07	1265.39	0.08	8.9E-01
<i>washc5</i>	293.53	-0.14	5.0E-01	141.55	-0.40	9.2E-04	143.95	-0.03	9.6E-01
<i>pxk</i>	205.36	0.19	2.9E-01	183.15	0.67	1.9E-04	120.35	0.65	7.3E-02
<i>hint1</i>	1719.70	0.28	2.6E-01	824.17	0.46	9.4E-03	336.79	-1.03	9.7E-03
<i>nsmce2</i>	260.89	-0.48	1.4E-04	79.51	-0.44	1.5E-02	82.97	-0.80	6.1E-02
<i>gimap2</i>	17.46	2.14	5.5E-04	46.44	0.04	9.5E-01	57.94	1.89	1.6E-02
<i>cdk5r1</i>	106.52	-0.59	3.7E-03	292.02	0.31	9.2E-02	7.22	-1.18	3.6E-01
<i>dph5</i>	344.39	0.51	2.8E-03	108.03	0.20	2.9E-01	63.25	-0.28	6.4E-01
<i>pdhb</i>	662.23	0.41	6.9E-03	2359.84	0.06	8.1E-01	680.86	-0.29	5.8E-01
<i>irf1</i>	5.62	0.32	7.6E-01	142.62	-1.19	2.9E-04	360.24	1.17	1.0E-01

Fig. 1.

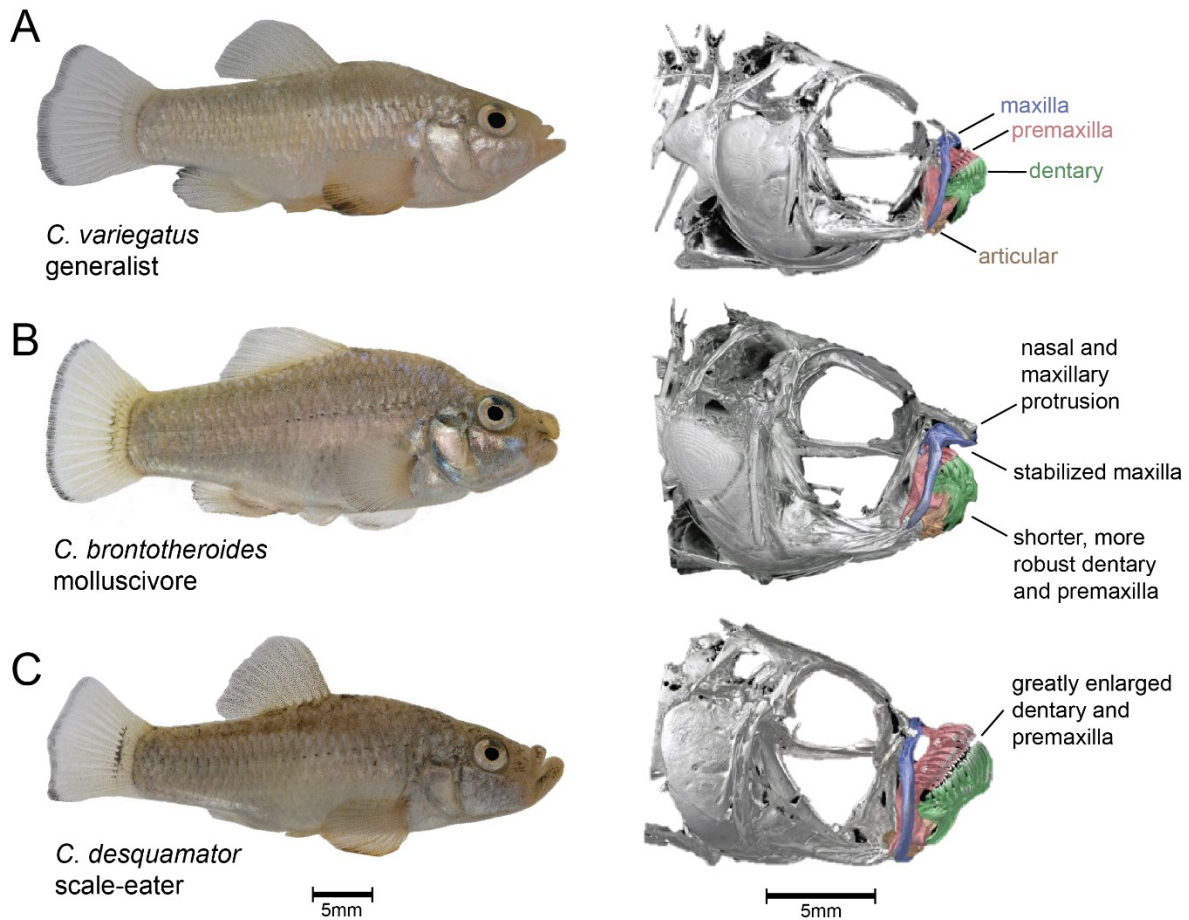


Fig. 1. San Salvador Island pupfishes exhibit exceptional craniofacial divergence despite recent divergence times. A) *Cyprinodon variegatus* (generalist), B) *C. brontotheroides* (molluscivore), C) *C. desquamator* (scale-eater). μCT scans modified from (Hernandez et al. 2018) show major craniofacial skeletal structures diverged among species including the maxilla (blue), premaxilla (red), dentary (green), and articular (brown).

Fig. 2.

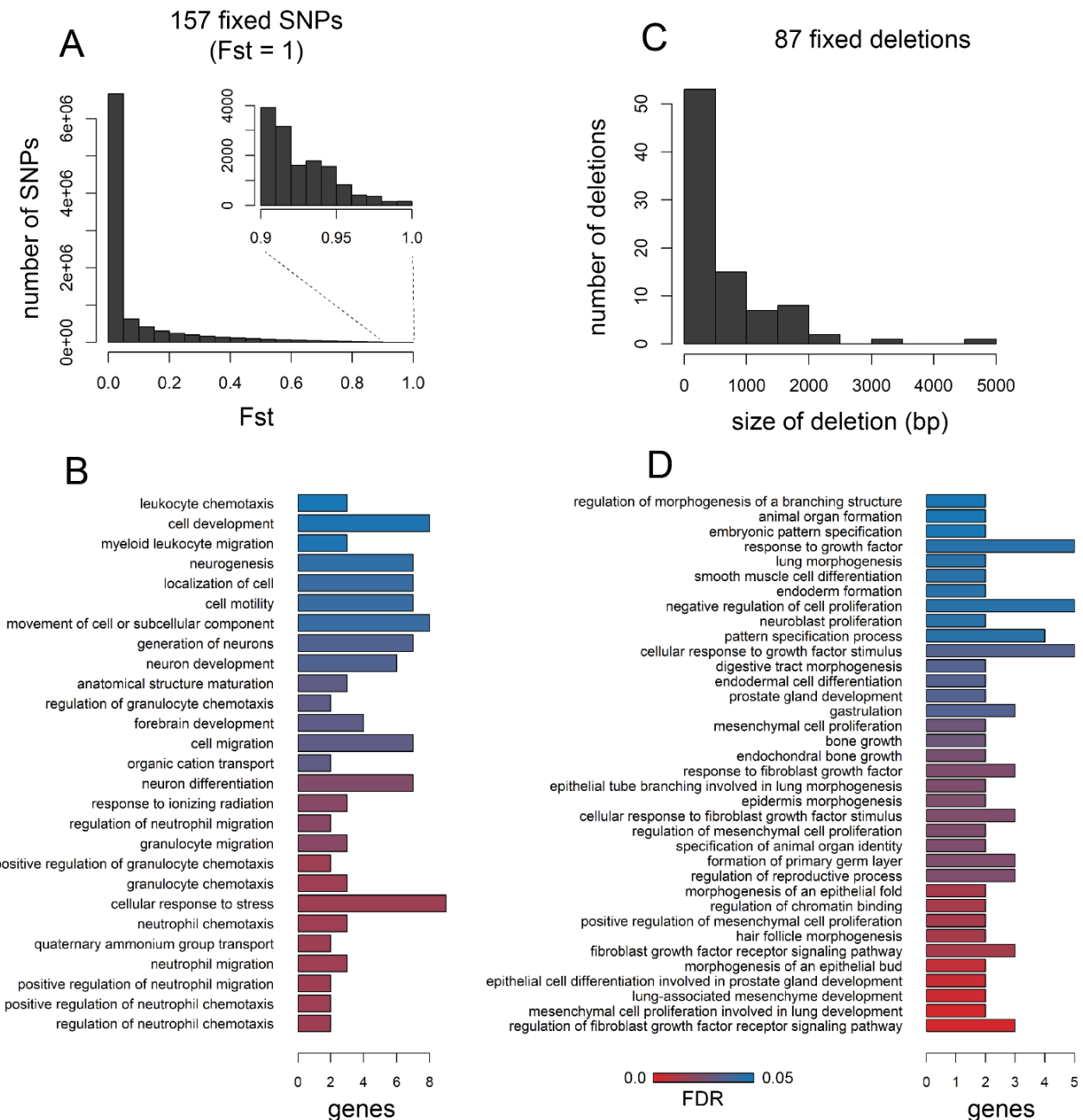


Fig. 2. Very few SNPs and structural variants are fixed between trophic specialists. A) Distribution of Weir and Cokerham *Fst* values across 9.3 million SNPs. 157 were fixed between species (*Fst* = 1). B) 46 of the 157 SNPs were located near 27 genes that were enriched for 27 biological processes (FDR < 0.05). C) Size distribution of the 87 deletions are fixed between species out of 80,012 structural variants. D) 34 of the 87 fixed deletions were within 10 kb of 34 genes that were enriched for 36 biological processes.

Fig. 3.

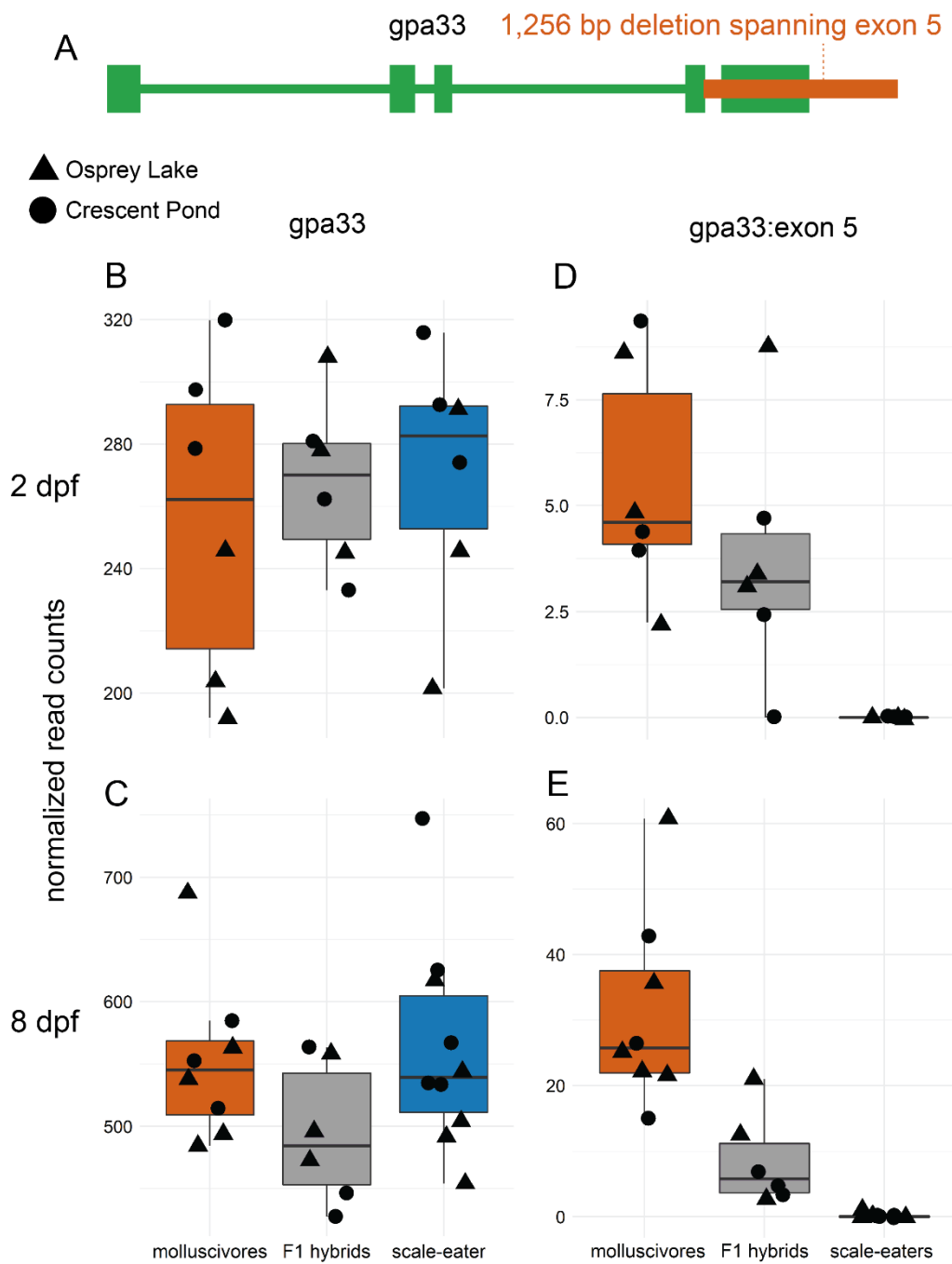


Fig. 3. The only fixed variant within a protein coding region is an exon deletion of *gpa33*.
 A) A 1,256 bp deletion (red) identified by DELLY spans the entire fifth exon of *gpa33* and is fixed in scale-eaters. B and C) The gene is not significantly differentially expressed between molluscivores (red) and scale-eaters (blue) at 2 days post fertilization (dpf) or 8 dpf when considering read counts across all exons ($P > 0.05$). D and E) However, when only considering the fifth exon, scale-eaters show no expression and F1 hybrids (grey) show reduced expression, supporting evidence for the deletion.

Fig. 4.

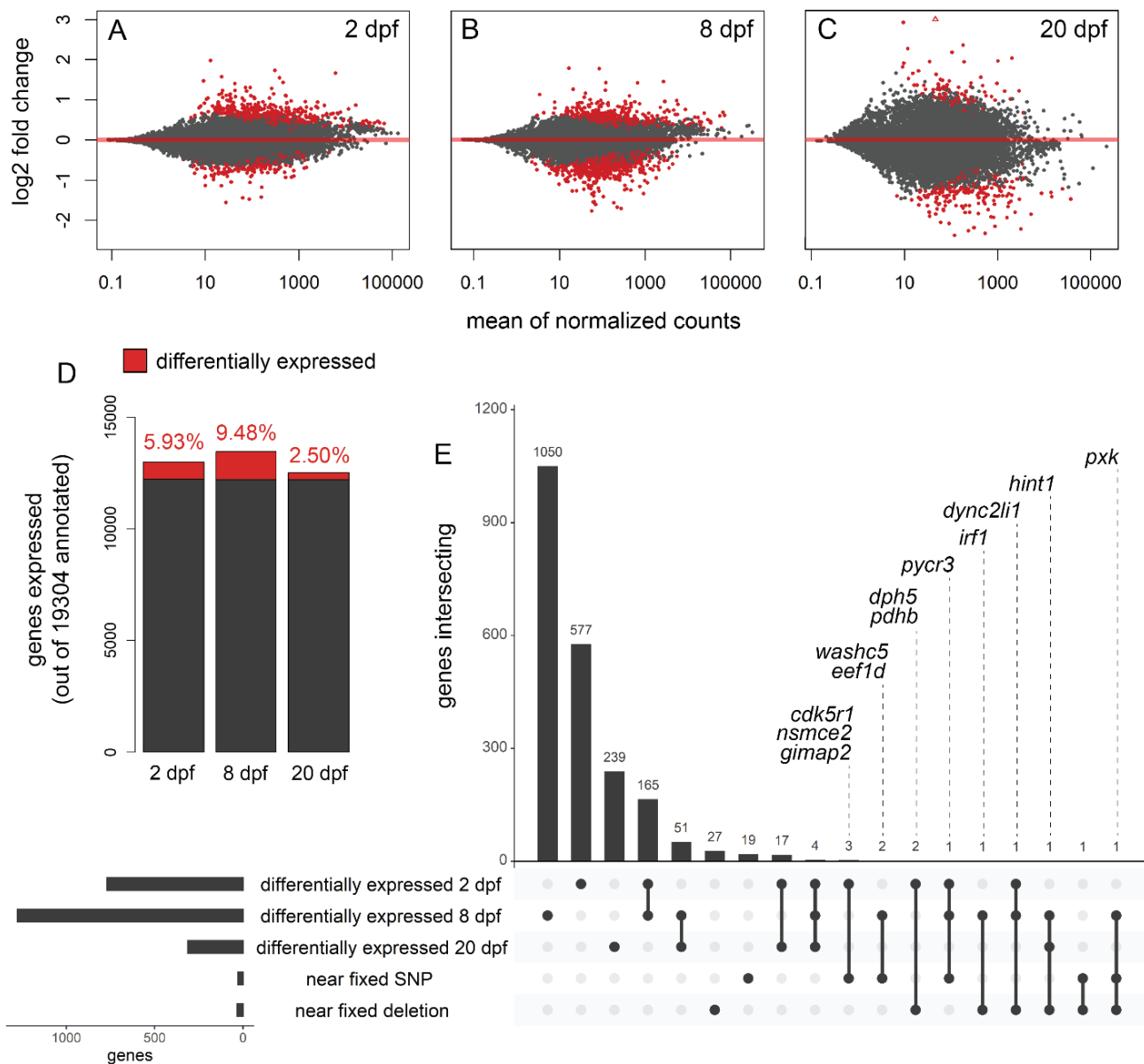


Fig. 4. Genes near fixed variants are differentially expressed between species across three developmental stages. Genes differentially expressed (red; $P < 0.01$) between molluscivores and scale-eaters at A) 2 days post fertilization (dpf), B) 8 dpf, and C) 20 dpf. Positive log₂ fold changes indicate higher expression in scale-eaters relative to molluscivores. D) Proportion of genes differentially expressed out of the total number of genes expressed across three stages. E) UpSet plot (Conway et al. 2017) showing intersection across five sets: genes differentially expressed at each of the three stages, genes within 10 kb of fixed SNPs, and genes within 10 kb of fixed deletions. The twelve labeled genes were differentially expressed during at least one stage and within 10 kb of fixed variants.

Fig. 5.

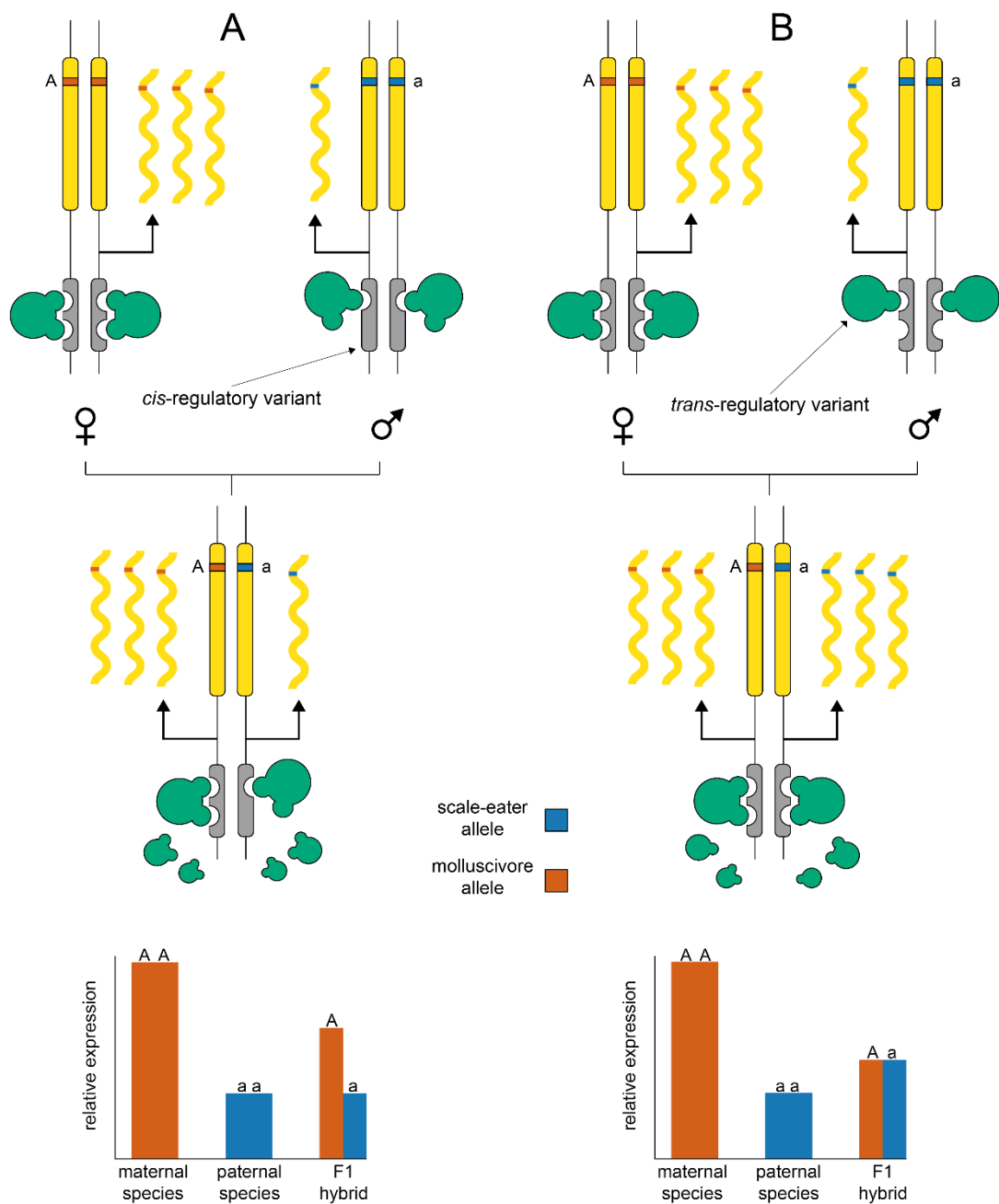


Fig. 5. Deciphering between *cis*- and *trans*-regulatory divergence influencing gene expression. Diagrams show protein coding gene regions (yellow) regulated by linked *cis*-acting elements (grey) and *trans*-acting binding proteins (green). In the examples, a female molluscivore is crossed with a male scale-eater to produce an F1 hybrid. The two species are alternatively homozygous for an allele within the coding region of a gene that shows higher expression in the molluscivore than the scale-eater. A) A *cis*-acting variant causing reduced expression results in low expression of the scale-eater allele in the F1 hybrid. B) Lower expression in the scale-eater is caused by a *trans*-acting variant, resulting in similar expression levels of both parental alleles in the F1 hybrid.

Fig. 6.

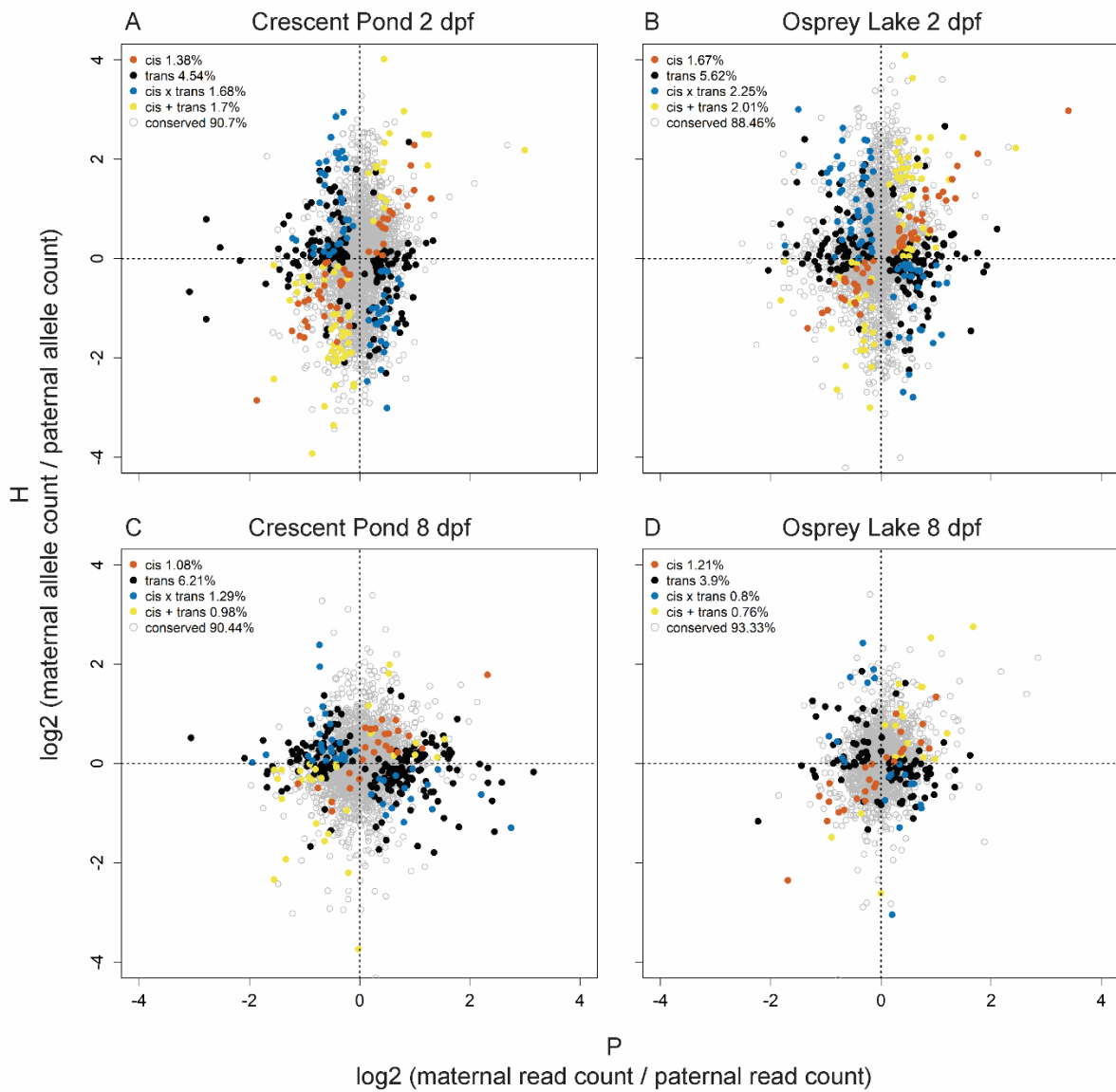


Fig. 6. Regulatory mechanisms underlying expression divergence between species. The ratio of maternal and paternal allelic expression in F1 hybrids (H) relative to the ratio of molluscivore and scale-eater gene expression in purebred F1 offspring (P) for genes containing heterozygous sites. Left panels show expression in Crescent Pond samples and right panels show Osprey Lake samples. Red = *cis* (significant ASE in F1 hybrids, significant differential expression between species, and no significant *trans*- contribution), black = *trans* (significant ASE in hybrids, significant differential expression between species, and significant *trans*- contribution), blue = *cis* \times *trans* (*cis* and *trans* effects show opposing signs, significant ASE, no significant differential expression between species, significant *trans*- contribution), yellow = *cis* + *trans* (*cis* and *trans* effects show the same sign, significant ASE, no significant differential expression between species).

species, significant *trans*- contribution), grey = conserved (No differential expression between species and no ASE).

Fig. 7.

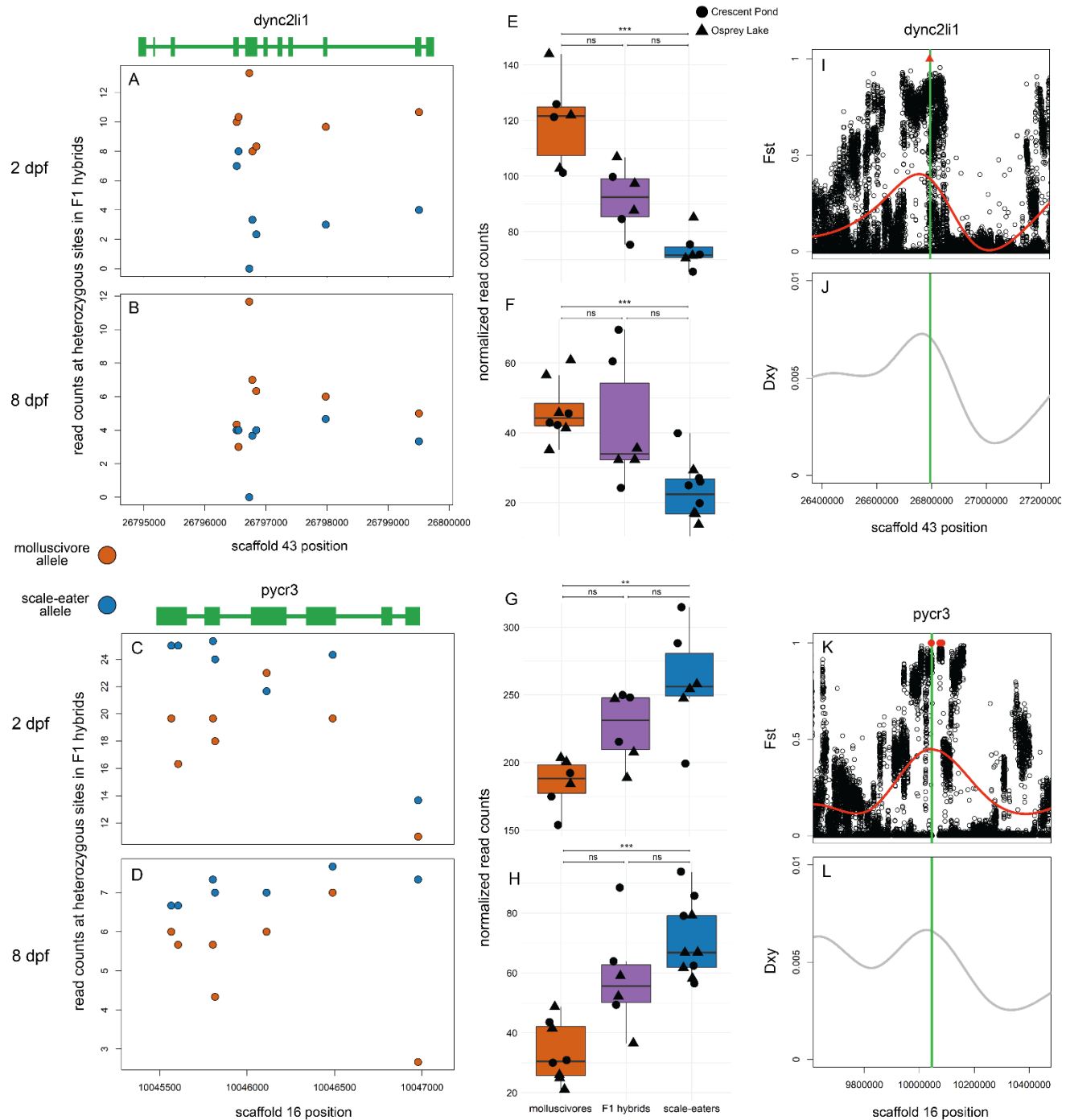


Fig. 7. Two genes near fixed variants show *cis*-regulatory divergence between trophic specialists. A-D) Mean counts for reads spanning *dync2li1* and *pycr3* that match parental alleles at heterozygous sites are shown for crosses between Crescent Pond molluscivores (red) and scale-eaters (blue) at 2 dpf (A and C) and 8 dpf (B and D). E-H) Normalized read counts for F1 offspring from Crescent Pond (circles) and Osprey Lake (triangles) crosses. Both genes are differentially expressed between molluscivores (red) and scale-eaters (blue) at both developmental stages and show additive inheritance in F1 hybrids (grey; $P < 0.01^*$, 0.001^{**} , 0.0001^{***} , $P > 0.01$ ns). For both genes, F1 hybrids show higher expression of alleles derived from the parental species that shows higher gene expression in purebred F1 offspring (MBASED $P < 0.05$) and show *cis*-regulatory divergence between species. I-L) Both genes (green lines) are within regions showing high relative genetic differentiation (Fst ; I and K) and high absolute genetic divergence (Dxy ; J and L). Red triangle shows fixed deletion. Red points show fixed SNPs ($Fst = 1$).

Fig. 8.

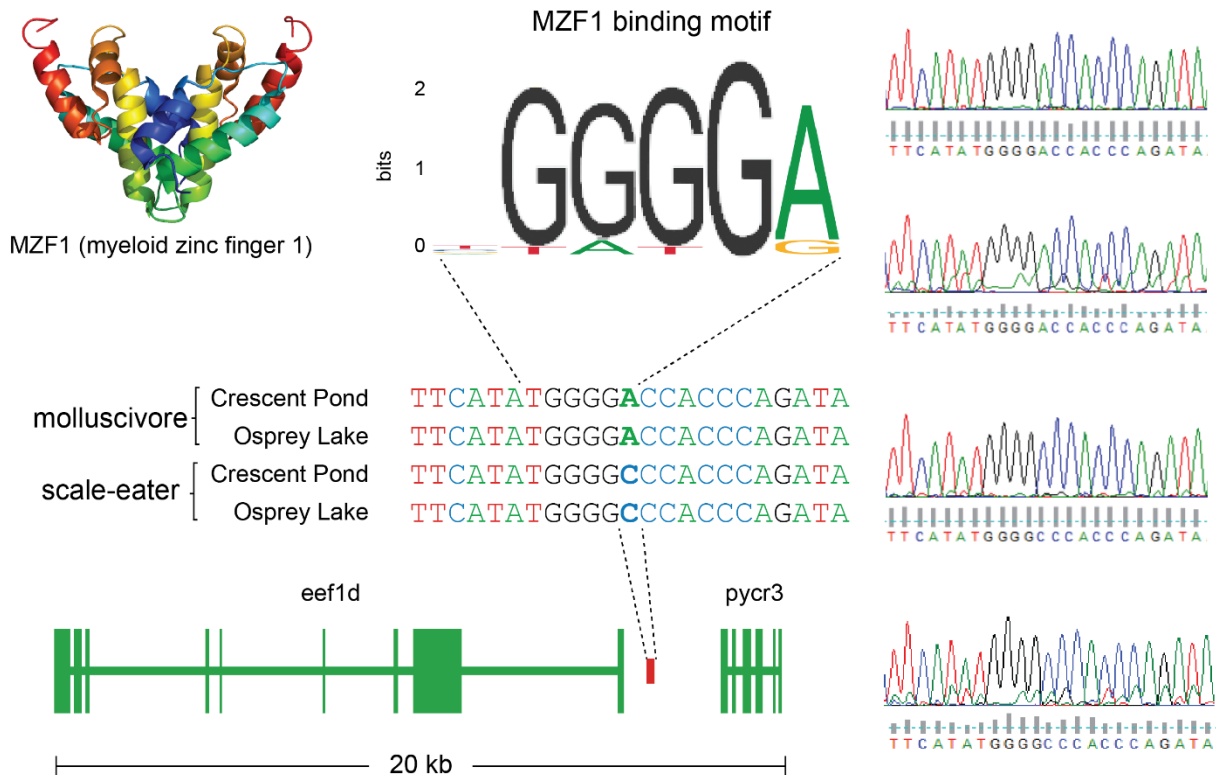


Fig. 8. Sanger sequencing confirms fixed SNP that could alter transcription factor binding near *pycr3*. Chromatograms on the right confirm the A-to-C transversion fixed in scale-eaters that falls between *eef1d* (Fig. S3) and *pycr3* (Fig. 7). The myeloid zinc finger transcription factor binds a motif that matches the molluscivore (JASPAR database matrix ID: MA0056.1), however, the scale-eater allele alters this motif.